ANL-ARC-228 Rev. 1

Neutronics Benchmark Specifications for EBR-II Shutdown Heat Removal Test SHRT-45R – Revision 1

Nuclear Engineering Division

ANL-ARC-228 Rev. 1

Neutronics Benchmark Specifications for EBR-II Shutdown Heat Removal Test SHRT-45R – Revision 1

---

prepared by
T. Fei, A. Mohamed and T. K. Kim
Nuclear Engineering Division, Argonne National Laboratory

January 23, 2013

SUMMARY

A neutronics benchmark specification was developed to support the analysis of SHRT-45R test, which was conducted in April 1986 using Experimental Breeder Reactor II (EBR-II) to demonstrate that a sodium-cooled fast reactor (SFR) with a sodium-bonded metallic fuel could be designed such that passive phenomena, as opposed to active electromechanical systems, are effective in protecting the reactor against the potentially adverse consequences of unprotected accidents.

This benchmark specification provides the data needed to construct neutronics models of the SHRT-45R test with any level of detail, including EBR-II reactor overview, geometry and dimensions of EBR-II subassemblies, compositions of fuel, coolant and structure at the beginning of SHRT-45R, fuel properties and operation conditions. The expected results from this benchmark are the reactor power distribution, decay heat parameters, and reactivity feedback coefficients for subsequent safety analysis of SHRT-45R transient.

.

Table of Contents

List of Tables

List of Figures

1 Introduction

The Shutdown Heat Removal Test (SHRT) program was carried out in EBR-II between 1984 and 1986. The objectives of this program were to support U.S. liquid metal reactors (LMR) plant design, provide test data for validation of computer codes for design, licensing and operation of LMRs, and demonstrate passive reactor shutdown and decay heat removal in response to protected and unprotected transients. The protected and unprotected transients tested include loss of flow in the primary and/or intermediate sodium loops as well as a loss of heat sink from the balance of plant. Additional tests were performed to examine the response of the system to balance of plant changes and others were performed to characterize reactivity feedbacks.

Passive safety in sodium fast reactors has been focused on making use of inherent reactor features during accidents to shut down the core, remove residual heat and keep the core cooled. In addition to the Doppler effect, negative reactivity feedback mechanisms based on thermal expansion and contractions of structural materials, and neutron leakage in the fast spectrum core can be used to passively shut down the core. Radial and axial core expansion, core flowering, and control rod driveline expansion are examples of these passive reactivity feedbacks. To keep the core cooled when forced circulation was lost, the natural circulation characteristics of sodium could be utilized through coolant density changes. Passive heat removal could be accomplished through use of natural convection, conduction and vessel wall radiation.

On April 3rd, 1986, SHRT-45R - a loss of flow test in which the plant protection system (PPS) was deliberately prevented from initiating a scram - was conducted to demonstrate the effectiveness of EBR-II's passive feedback mechanisms. During the test, which was conducted starting from full power and flow, both the main primary and intermediate-loop coolant pumps were simultaneously tripped to simulate an unprotected loss-of-flow accident. Temperatures in the reactor quickly rose to a high, but acceptable, level as the passive reactivity feedbacks shut the reactor down safely.

SHRT-45R occurred at the end of EBR-II Run 138B. Prior to Run 138-B, EBR-II was shut down for approximately a month and a half. Run 138B was conducted for 5.67 days: it was started up and operated at 17.9 MW for 4.03 days and the power level was increased to 60.0 MW for 1.64 days for a total of 177 MW-days. Accordingly, it is assumed that prior to that start of SHRT-45R, EBR-II was operated at full power and full flow. In addition, just prior to test initiation, the control rod drives were deactivated to preclude control rod movement during the transient period. This action prevented insertion or withdrawal of the rods by the drive motors, but it did not affect the scram function. In order to protect the reactor from equipment failures during testing, special scram protection was implemented just prior to test initiation.

The SHRT-45R transient was initiated by a trip of the primary and intermediate pumps which was accomplished by opening the 2400 V breaker powering the motor-generator (M-G) set and thus removing the power supply from the pumps. Each primary pump had its own controller and M-G set. To obtain the desired flow coastdown, energy was taken out from the motor of the M-G set at the beginning of the coastdown and applied at the end of the coastdown through the coupling and decoupling of the motor-generator (M-G) set clutch, which retained its power supply. An auxiliary electromagnetic pump in the primary loop continued to receive power from its battery while the rectifier remained tripped, as would occur during a total station blackout. As the SHRT-45R test continued, the reactor power decreased due to reactivity feedbacks. Once the test was initiated, no automatic or operator action took place until the test had concluded, at which point the reactor was scrammed.

The benchmark specifications of EBR-II's SHRT-45R provided in this report address the benchmarking definition requirements for collaborative efforts within international partnerships on the validation of simulation tools and models in the area of sodium fast reactor (SFR) passive safety. Validated tools and models are needed to evaluate SFR passive safety phenomena as well as to produce reactor designs that incorporate these passive features into the system's response to accident initiators. Comparison with experimental data creates unique opportunities to improve SFR computational codes and methods. Further, U.S. participation in this benchmark collaboration will benefit SFR development and design by providing an opportunity for the validation of computational methods while increasing knowledge of and experience with passive safety features and characteristics of fast reactors.

An overview of the EBR-II reactor is given in Chapter 2 followed by detailed descriptions of the reactor core geometry, material compositions and fuel properties in Chapter 3. Chapter 4 provides the expected results of the SHRT-45R benchmark.

2 EBR-II Plant Overview

The EBR-II plant was designed and operated by Argonne National Laboratory for the U.S. Department of Energy. Operation began in 1964 and continued until 1994. EBR-II is a heterogeneous, sodium cooled fast breeder reactor designed to produce a thermal power of 62.5 MW with an electric output of approximately 20 MW.

The EBR-II reactor vessel and its components are illustrated in Figure 2.1. The vessel grid-plenum assembly accommodated 637 hexagonal subassemblies (S/A's). The grid is divided into three main regions: core, inner blanket (IB) and outer blanket (OB). Figure 2.2 illustrates the subassembly arrangement of the reactor and the subassembly identification convention. Each subassembly position was identified by a unique combination of three parameters: row, sector and position within the sector. Subassembly row identification begins at Row 1 at the subassembly in the core-center and moves outward to Row 16. Row 1 had one subassembly. Row 2 had six subassemblies. From Row 2 outward to Row 14, each row had 6 more subassemblies than the last. Rows 15 and 16 were not complete rows and had 66 and 24 subassemblies, respectively.

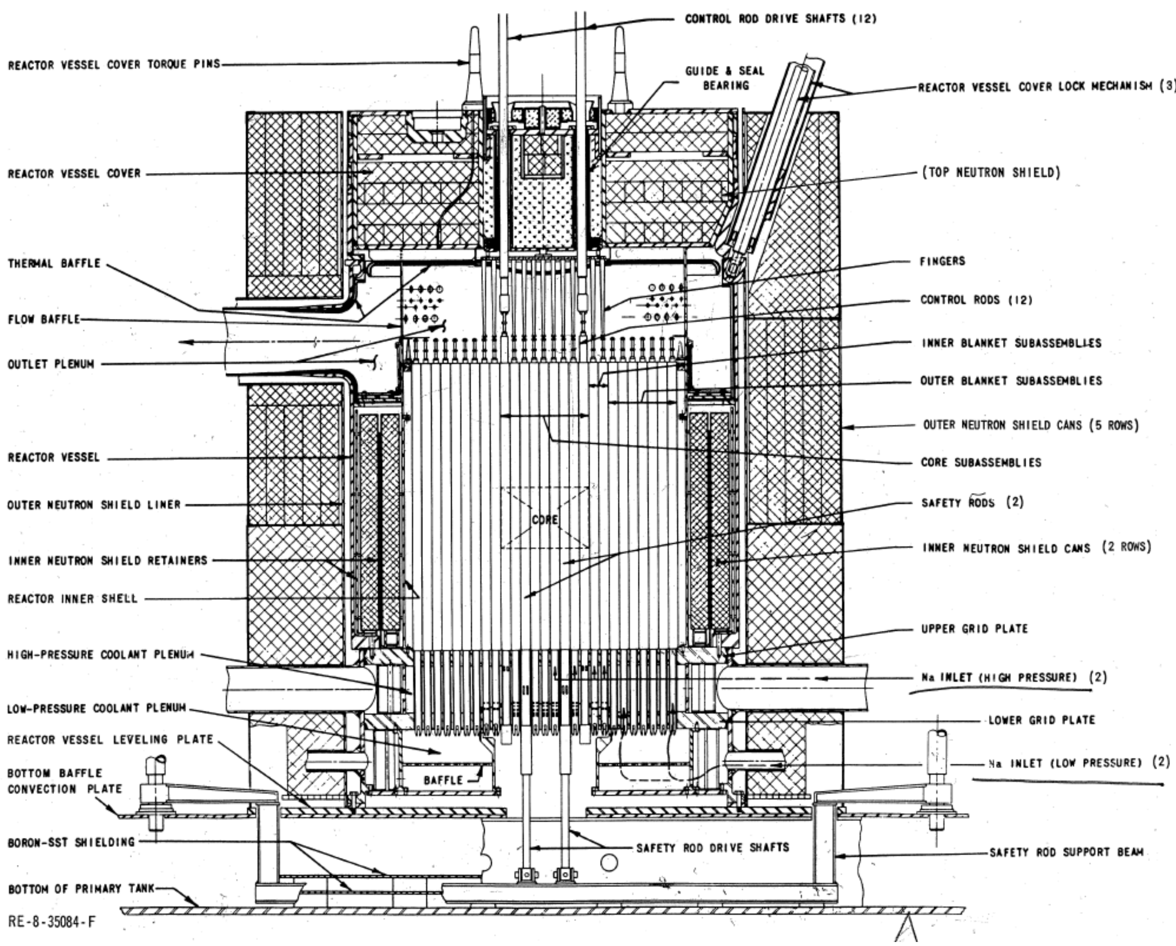

Figure 2.1. EBR-II Reactor Vessel and Neutron Shield Assembly

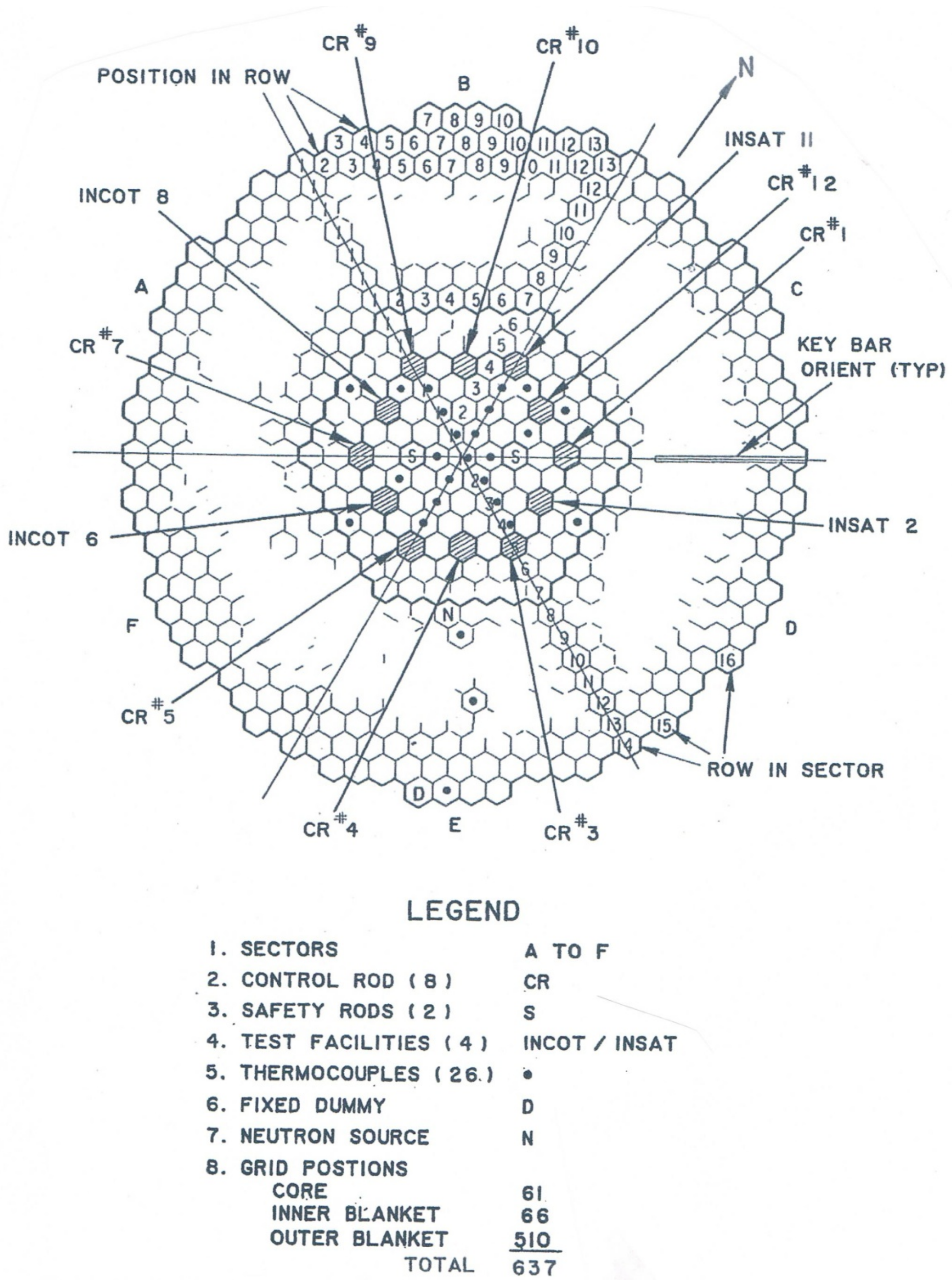

Figure 2.2. EBR-II Core Layout

Each row was broken up into six sectors A through F. As each row approximated a hexagon, each side of the row was assigned to one of the six sectors. The final parameter needed to identify a subassembly position is the position within the sector. The line of subassemblies dividing sectors A and F were defined as the subassemblies in position 1 of their respective rows within sector A. The line of subassemblies that divide sectors A and B are therefore defined as the subassemblies in position 1 of their respective rows within sector B. This pattern continues for the remaining four sides of the core layout. As an example, the subassembly labeled as CR

#10 in Figure 2.2 is positioned in subassembly location 5B3, where 5 is the row, B is the sector and 3 is the position within the sector.

The central core comprised the 61 subassemblies in the first five rows. Two positions in row 3 contained safety-rod subassemblies, and eight positions in Row 5 contained control-rod subassemblies. Two positions in Row 5 contained the instrumented subassemblies (INSAT) XX09 and XX10, and one position in Row 5 contained the in-core instrument test facility (INCOT) XY-16. The remainder of the central core region contained driver fuel or experimental-irradiation subassemblies.

The inner blanket region was composed of Rows 6 and 7. Originally these rows were loaded with blanket subassemblies. But for SHRT-45R, no blanket subassemblies were loaded in this region. Instead, the inner blanket region contained the reflector subassemblies of Row 7 and the driver-fuel and irradiation subassemblies of the expanded core. The outer blanket region comprised the 510 subassemblies in Rows 8-16, which were either blanket or reflector subassemblies.

EBR-II was heavily instrumented to measure mass flow rates, temperatures and pressures throughout the system. While several instruments failed prior to the shutdown heat removal tests, a large number of measurements are available throughout the system to compare benchmark simulation results against experimental data.

EBR-II was heavily instrumented to measure mass flow rates, temperatures and pressures throughout the system. While several instruments failed prior to the shutdown heat removal tests, a large number of measurements are available throughout the system to compare benchmark simulation results against experimental data. Measurements are also available for the fission power during the transient. However, because these measurements only cover fission power, decay heat production will need to be estimated for the transient to produce the total transient power.

3 EBR-II Reactor Core

The EBR-II reactor core configuration for SHRT-45R is depicted in Figures 3.1 and 3.2 which provide various illustrations of the core-loading pattern for Run 138B. Figure 3.1 shows a schematic of core-loading pattern while Figure 3.2 shows the actual subassemblies in the first 8 rows.

During Run 138B, a large variety of subassembly types were utilized: driver, blanket, reflector, dummy, experimental, control and safety. Two types of driver subassemblies were used for Run 138B. The first was the MARK-II fuel manufactured by Atomics International (AI), denoted as MARK-II AI. It is referred to in Figure 3.2 as MK2AI. The second driver type was MARK-IIA fuel, referred to in Figure 3.2 as MK2A.

Several variations of the basic driver subassemblies were also used. In addition to the standard MARK-IIA and MARK-II AI subassemblies, partial driver subassemblies in Figure 3.1 with approximately half of the fuel elements replaced with dummy elements were used. High-flow drivers (HFD) were the same as standard driver subassemblies but with extra inlet flow holes drilled in the subassembly inlet nozzle to allow for high coolant flow.

In Figure 3.2, dummy subassemblies are identified as ‘K’ (e.g. K013). Control-rod subassemblies are identified as either ‘CONTROL’ or ‘HW CNTR,’ which refers to high-worth control rod design subassembly option. Subassemblies X320C, X411 and X412 were experimental-irradiation subassemblies. EBR-II was loaded with four test facility subassemblies for Run 138B: XY-16, XX09, XX10 and LUM-2. XY-16 was a dummy subassembly. XX09 and XX10 were instrumented subassemblies (INSATs) and LUM-2 was closest to the K-type dummy subassemblies. Figure 3.2 lists one subassembly in Row 4 as C2776A XETAGS. This subassembly was a MARK-II AI subassembly with Xenon tag gas. The subassembly designated as S1951 in row 8 of Figure 3.2 was a neutron source assembly and is treated as stainless steel reflector subassembly for this benchmark.

Reflector subassemblies are identified as ‘SSR’ in Figure 3.2. The remaining subassemblies in Rows 11-16 were depleted uranium outer blanket subassemblies. Table 3.1 summarizes the different types of subassemblies in the core loading for SHRT-45R. It should be noted that the inner blanket region did not contain any blanket assemblies. It was named as such because it originally housed blanket subassemblies. The whole core configuration of Run 138B was surrounded by a sodium pool.

3.1 Subassembly Geometry

The outer configuration of all subassemblies was very similar as highlighted by a MARK-II fuel assembly in Figure 3.1.1. In general, all assemblies could be divided into three main sections: (1) The upper adapter was formed to fit the top of the hexagonal outer tube of the central region and the top part of the upper adapter was slotted to adjust the orientation of the subassembly within the reactor grid; (2) the center region of each subassembly was surrounded by a hex tube, which acted as a protective sheath for the subassembly. This tube also channeled the coolant past the material contained in the subassembly, and (3) the lower adapter positioned the subassembly within the reactor grid and determined the amount of coolant flow through the subassembly. Subassemblies that were to be positioned in Rows 1 through 5 had core-type lower adapters. The expanded core-type lower adapter was used for driver fuel and irradiation subassemblies located in Rows 6 or 7 of the reactor. Furthermore, the outer blanket lower adapter was used for subassemblies in Rows 8-16.

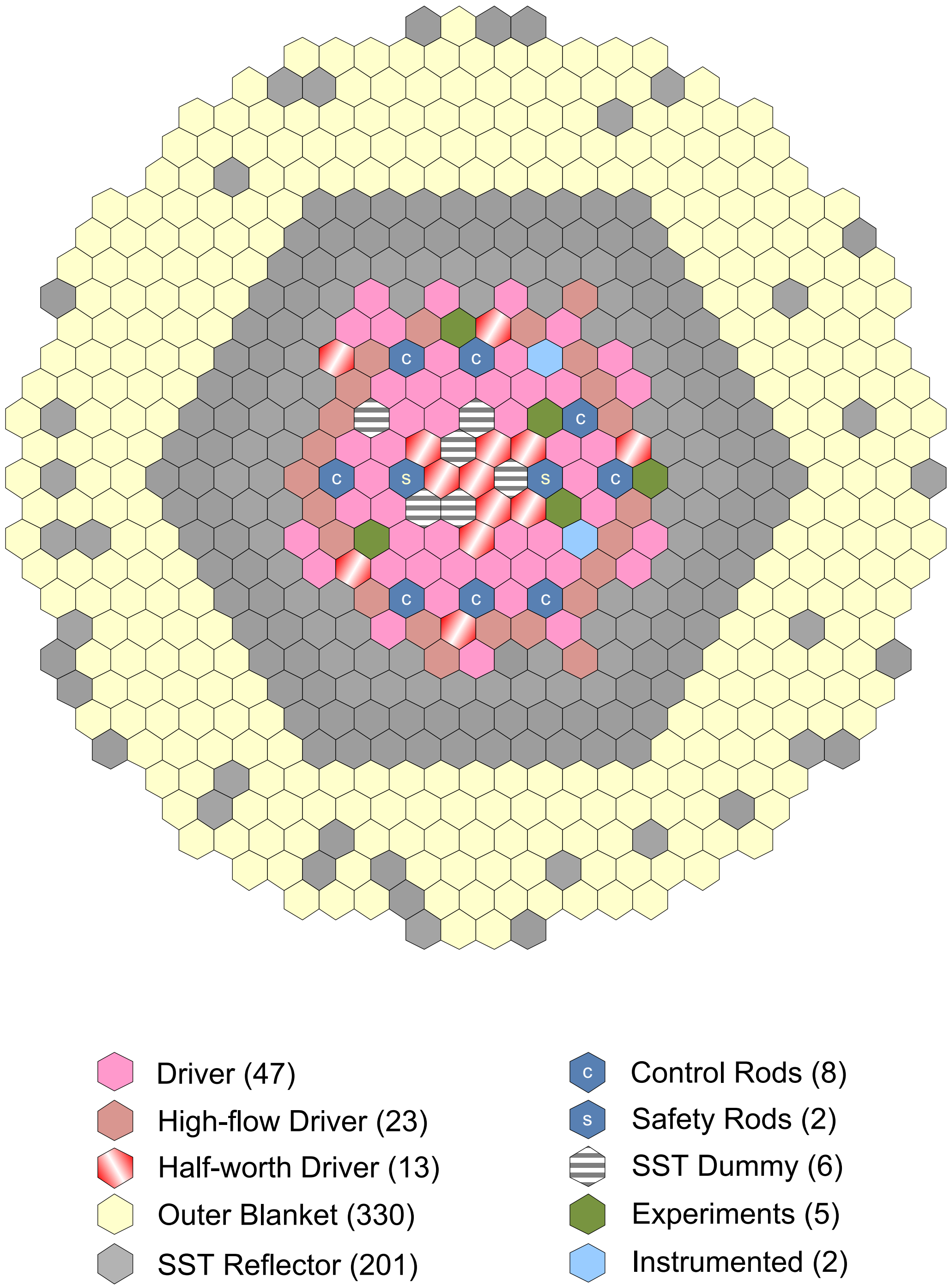

Figure 3.1. Schematic of EBR-II Subassembly Core Loading Pattern for Run 138

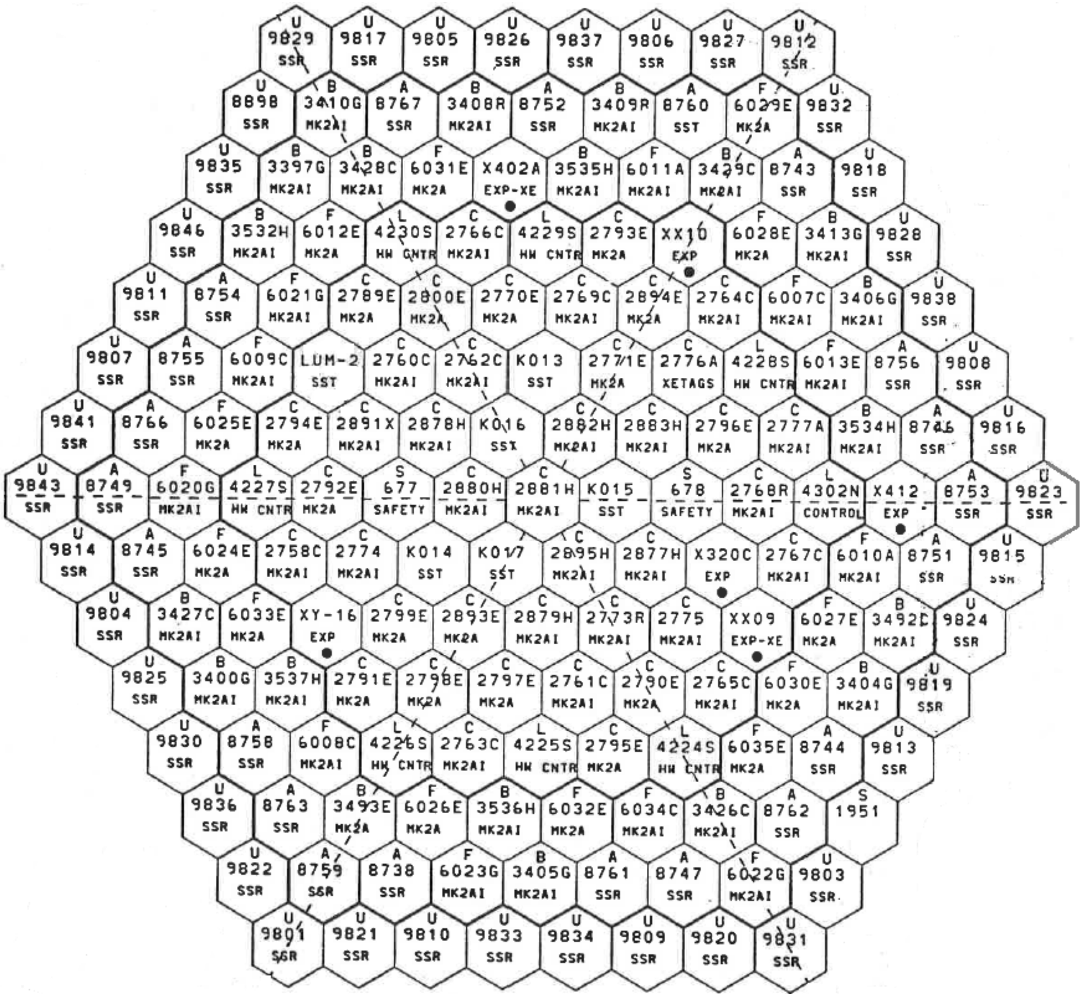

Figure 3.2. Actual Core Loading Pattern (First 8 Rows)

Table 3.1. SHRT-45R Types of Subassemblies

Subassembly Type	Figure 3.1 Identifiers	Figure 3.2 Identifiers
MARK-II AI		MK2AI
MARK-IIA		MK2A
Stainless Steel Dummy		K SST, LUM-2 SST
Stainless Steel Reflector		A SST, U SST
Outer Blanket		N/A
Control		CONTROL, HW CNTR
Safety		SAFETY
Instrumented		XX09, XX10
Experimental		XY-16, X320C, X402A, X412, XETAGS

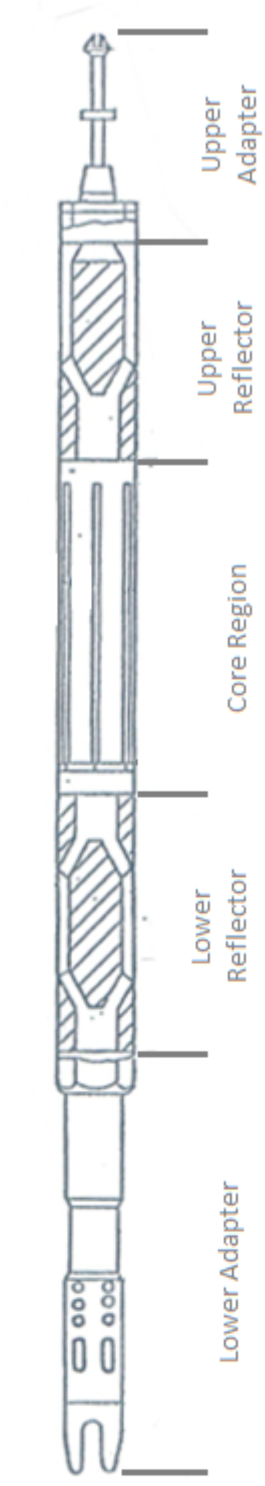

Figure 3.1.1. Sample MARK-II Subassembly Configuration

The inner configuration of the center section of a subassembly varied depending upon the specific subassembly type. Figure 3.1.1 shows an isometric view of the inner configuration of a MARK-II subassembly. The center section of the MARK-II subassembly consisted of an upper shield, a core bundle of fuel elements and a lower shield. For each subassembly type, geometric details are provided in the following subsections of the inner configuration of each of the different types of subassemblies loaded in the reactor core for the SHRT-45R test. For those subassembly types that include a core bundle of fuel elements, Tables 3.1.1 and 3.1.2. present the nominal design parameters of the subassembly element by type. These tables give design data for the wire-wrapped cladded fuel elements for a number of bundle element designs used in Run 138B.

The MARK-II and MARK-IIA fuel elements were part of the central core driver and internal blanket driver subassembly designs. In both Tables 3.1.1 and 3.1.2, the numbers in parentheses are for the MARK-IIA fuel element. All the other numbers in the columns are common to both the MARK-II and the MARK-IIA designs. The MARK-IIS element was used in the high worth control rod design while the MARK-IIC was utilized in the safety rod design. Each fuel element clad tube contained a single metal fuel slug. U-5 wt. % Fs (U-5Fs) is the fissium fuel alloy uniquely developed and fabricated for the ANL EBR-II reactor. For the purposes of this benchmark exercise, the relevant material properties of the fissium fuel are provided in Section 3.2.1. Figure 3.1.2 show schematics of plane sections in driver, half-worth driver, 61-pin fuel, and blanket assemble.

Table 3.1.1. Design Parameters of EBR-II Subassembly Elements at 20 °C

Item	Mark-II(A)	Mark-IIS (C)	XX09	XX10	Outer Blanket
Fuel alloy, wt. %	U-5Fs	U-5Fs	U-5Fs	Stainless Steel	Depleted Uranium
Enrichment weight, % ^{235}U	67	67	67	N/A	~ 0.0
Number of Elements	91 (91)	61	59 of 61	18 of 19	19
Fuel-slug length, m	0.3429	0.3429	0.3429	N/A	1.3970
Fuel-slug diameter, mm	3.3655	3.3655	3.3655	N/A	11.0998
Cladding-wall thickness, mm	0.305	0.305	0.305	Solid rod	0.4570
Cladding-wall OD, mm	4.4196	4.4196	4.4196	8.81	12.5222
Element length, m	0.6108 (0.6362)	0.5334 (0.6108)	0.6108 (0.6494)	0.6108 (0.6951)	1.575
Restrainer height above fuel, mm	12.7	12.7	None	None	N/A
Sodium level above fuel, mm	31.75 (6.35)	6.35	6.35	6.35	30.48
Plenum gas	Inert gas	Inert gas	Inert gas	Inert gas	N/A
Cladding material	316SS	316SS	316SS	316SS	304SS
Space-wire diameter, mm	1.24	1.24	1.24	1.24	None
Space-wire material	316SS	316SS	316SS	316SS	N/A

Table 3.1.2. Design Parameters (at 20°C) of EBR-II Subassembly Structure

	Mark-II/ Mark-IIA	XX09/XX10	Safety/HWCR	Reflector/ Uranium Blanket
Pitch, mm	58.929	58.929	58.929	58.929
Outer Hex Tube, mm				
Flat-to-flat outside	58.166	58.166	58.166	58.166
Flat-to-flat inside	56.134	56.134	56.134	56.134
Material	316SS	304SS	316SS	304SS
Outer Hex Tube, mm				
Flat-to-flat outside		48.4	48.4	
Flat-to-flat inside		46.4	46.4	
Material		304SS	304SS	
Upper adapter/fixture	304SS		304SS	304SS
Upper axial shield	304SS		304SS	
Lower axial shield	304SS		304SS	
Lower adapter	304SS		304SS	304SS

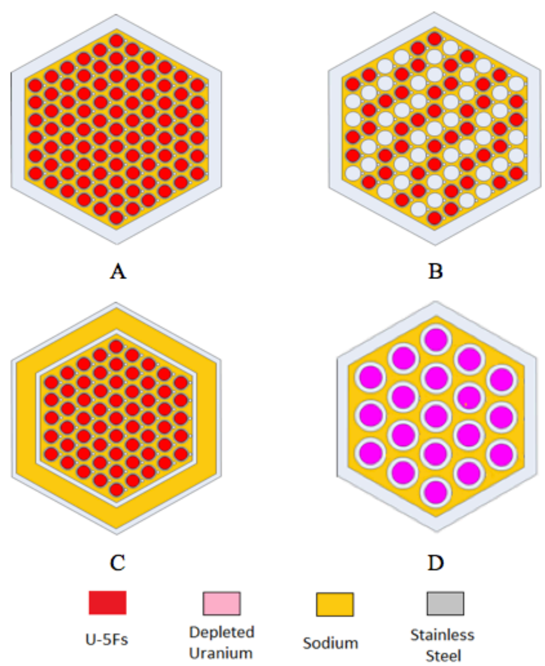

Figure 3.1.2 Schematic of Assembly Plan Views: (A) 91-Pin Driver, (B) 45-Pin Half-worth Driver, (C) 61-Pin Fuel and (D) Blanket Assembly

Details of all subassembly types used in EBR-II Run 138B are provided in Appendix A. Further information can be found in the accompanying document of the systems and safety analysis part of the benchmark specifications.

3.1.1 Control Rod/Safety Rod positions

There were eight control subassemblies located in row 5 of the reactor. Each consisted of a hexagonal tube, called a guide thimble, and a control rod. The control rod was designed to be moved vertically 43.815 cm (17.25 in.) within the guide thimble. The control rod contained fuel elements in the approximate center of the control rod subassemblies.

In the High-worth Control Rod (HWCR) design version of the control rod, the fuel element pin bundle was located below a boron carbide poison pin bundle section. This poison section in the HWCR entered the core region when the fuel element pin bundle section was lowered out of the core. Conversely when the fuel pin bundle section was raised back into the core, this boron pin poison section was raised out of the core, which therefore maximized the reactivity swing. There was a single control rod designated as CONTROL in Figure 3.2 which did not have B_4C absorber at position 3D1 and was similar in design to the MARK-IIC safety rods. For SHRT-45R the control rod insertion depth at the beginning of the test was such that the bottom of the control rod fuel bundle was 21.06 cm below that of the fuel bundle of the core driver subassemblies as shown in figure 3.1.1.1 below.

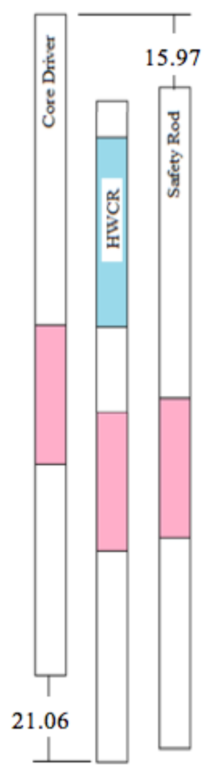

Figure 3.1.1.1 Relative Positions of Driver, HWCR and Safety Rods

There were two safety subassemblies located in row 3 of the reactor, each of which consisted of a safety rod contained in a hexagonal guide thimble. The guide thimble was similar in outward configuration to the other subassemblies used in the reactor and was semi-permanently installed and secured to an adapter on the reactor lower grid plate. This hexagonal section of the safety rod contained 61 fuel elements located in the approximate center of the rod subassembly.

The safety rod was normally positioned in the reactor with the fuel elements either at the same elevation as the core region or 36.195 cm (14.25 in.) lower than the core region to position the fuel element outside the core region. For SHRT-45R the safety rod insertion depth at the initiation of the test was such that the bottom of the safety rod fuel bundle was 15.97 cm below that of the fuel bundle of the core driver subassemblies. The positions of both safety and control assemblies are different from that given in the original report due to a change in the axial base plane.

3.1.2 Experimental Subassemblies

In EBR-II Run 138B, the experimental subassemblies that were loaded into the core consisted of XY-16, X320C, X402A, X412 and C2776A (XETAGS). Subassembly XY-16 had 61 solid Type 304 stainless steel wire-wrapped dummy MARK-II elements. In line with using a control rod position, the dummy element was located in the inner hexagon tube within the guide thimble.

The experimental subassembly X320C was a large specimen structural irradiation subassembly. It had a specimen cage of a Westinghouse design steel fixture with no coolant flow and for the purposes of this benchmark will be modeled as Stainless steel dummy K assemblies. On the other hand, X402A and X412 were both 91-pin MARK-IIA fuel element bundle qualification tests. C2776A (XETAGS) was a MARK-II AI subassembly with Xenon tag gas.

3.2 Core Data

In addition to the core loading of the different types of subassemblies that have been given in earlier sections, data is provided below regarding subassembly compositions. For HWCR poison pins, the B4C density is 2.40g/cc.

3.2.1 Fuel Composition

As mentioned earlier, the various driver and blanket assemblies were partially depleted prior to SHRT-45R. Table 3.2.1 summarizes homogenized core fuel compositions of the fuel section of the half-worth driver at the central core position 1A1 at 20 ^{o}C, depleted for 3 equal segments of the fuel section of the subassembly (1 being the lower section, 2 the middle, and 3 the upper section). It should be noted that axial fuel swelling of 6.88% corresponding to 4.5 at. % average core burnup is included in the fuel height used in the calculation of these homogenized number densities.

In this Table, LFP:U^{235} designates the atom number density of the lumped-fission-products resulting from U^{235} fission. Similar number densities of lumped-fission-products from fission in U^{238}, Pu^{239}, Pu^{240} and Pu^{241} are also included. However, La^{139} and Nd^{148} were not included in the fission products' lumps so that chemistry testing at different intervals over the life of a given assembly would validate its composition and burnup.

Table 3.2.1. Isotopic Compositions (# atoms/barn.cm at 20°C) for Core Assembly 1A1

Isotope	1A1		
	Half-worth Driver		
	1	2	3
U^{234}	8.32093E-08	9.89179E-08	7.19888E-08
U^{235}	3.45384E-03	3.44914E-03	3.46752E-03
U^{236}	1.75723E-05	1.73345E-05	1.53748E-05
U^{238}	1.74866E-03	1.74815E-03	1.74958E-03
NP^{237}	1.29516E-07	1.44909E-07	1.06755E-07
Pu^{236}	8.46741E-14	1.14073E-13	6.06560E-14
Pu^{238}	7.61553E-10	8.29154E-10	5.60322E-10
Pu^{239}	4.88128E-06	4.86669E-06	4.27091E-06
Pu^{240}	8.72197E-09	7.98951E-09	6.70047E-09
Pu^{241}	1.31241E-11	1.15727E-11	8.79862E-12
Pu^{242}	1.38488E-14	1.20708E-14	8.03667E-15
Am^{241}	4.54547E-14	4.02155E-14	2.99136E-14
Am^{242m}	3.23745E-17	2.80712E-17	1.86655E-17
Am^{243}	1.04172E-17	8.68971E-18	5.38622E-18
Cm^{242}	1.00274E-16	8.69318E-17	5.77991E-17
Cm^{243}	3.16120E-20	2.40150E-20	1.63679E-20
Cm^{244}	1.79030E-20	3.55805E-21	2.20573E-21
Cm^{245}	4.07167E-24	4.02992E-25	2.79743E-25
Cm^{246}	3.59919E-28	2.35608E-29	1.51737E-29
LFP:U^{235}	2.94226E-04	2.99156E-04	2.82825E-04
LFP:U^{238}	2.52970E-06	2.97870E-06	2.18368E-06
LFP:Pu^{239}	7.34811E-08	7.92980E-08	5.55484E-08
LFP:Pu^{240}	3.27430E-11	3.41801E-11	2.13305E-11
LFP:Pu^{241}	1.09960E-13	1.02202E-13	6.30781E-14
La^{139}	1.89360E-05	1.92820E-05	1.81756E-05
Nd^{148}	5.01357E-06	5.10645E-06	4.81320E-06
Fissium	6.71053E-04	6.71053E-04	6.71053E-04

Table 3.2.2 gives the fissium isotopic composition for the U-5 wt. % Fs MARK-II fuel. It is noted that the 5% fissium composition in addition to the sodium, stainless steel (clad, wire-wrap and duct) should be added to the composition in Table 3.2.1 to form the assembly homogenized compositions of the fuel section for a given assembly. Similar tables are given in Appendix B and C for all core fueled assemblies (driver, half-worth drivers, control- and safety-rods, experimental, and XX09) and blanket assemblies.

Table 3.2.2. U-5Fs Isotopic Composition

Material	Weight %
Uranium	95.0
Zirconium	0.10
Molybdenum	2.46
Ruthenium	1.96
Rhodium	0.28
Palladium	0.19
Niobium	0.01

Table 3.3. Design and Operating Data for EBR-II Run 138B

GENERAL	
Heat output (design/operating), MW	62.5/60.0
Gross electrical output, MW	20.0
Primary sodium temperature to reactor °C	343
Primary sodium temperature from reactor, °C	443
Average coolant temperature in core, °C	393
Primary sodium flow rate, Liters/sec	566
Primary system sodium capacity, Liters	340 000
Secondary sodium temperature to heat exchanger, °C	289
Secondary sodium flow rate, Liters/sec	345
Average core temperature, °C	
Fuel	487
Steel	412
Coolant	393
REACTOR DATA	
Core dimensions	
Equivalent diameter, cm	35.10
Core height, 0 at. % burnup, cm	34.29
Core height, 4.5 at. % burnup, cm	36.65
Upper- and lower-reflector dimensions, cm	
Equivalent outer diameter	69.72
Axial height of upper reflector	38.9
Axial height of lower reflector	57.2
Radial reflector dimensions, cm	
Equivalent outer diameter	101.9
Radial thickness	16.1
Axial length	139.7

Radial blanket dimensions, cm	
Equivalent outer diameter	156.2
Radial thickness	27.15
Axial length	139.7
Driver fuel assembly dimensions (at 20°C), cm	
Fuel-element type	MARKIIA and MARKII AI
Element length MARK-II AI/MARK-II A	61.08/63.62
Restrainer height above fuel	1.27
Sodium level above fuel	3.175
Plenum volume, cm^3	2.41
Plenum gas	Helium
Cladding material	SS316
Space-wire material	SS316
Number of pins per assembly	91
Outer cladding diameter	0.4420
Inner cladding diameter	0.3810
Outer fuel diameter	0.3366
Wire wrap diameter	0.1245
Fuel-pin length, 0 at. % burnup	34.29
Fuel-pin length, 4.5 at. % burnup, cm	36.65
Bond	Sodium
Volume fractions (%)	
Fuel alloy	26.92
Stainless steel (Type 316)	22.29
Sodium	50.79
Control- and safety assembly dimensions (at 20°C), cm	
Fuel-element type	MARKII AI
Number of pins per assembly	61
Outer cladding diameter	0.4420
Inner cladding diameter	0.3810
Outer fuel diameter	0.3366
Wire wrap diameter	0.1245
Volume fractions (%)	
Fuel alloy	18.04
Stainless steel	22.69
Sodium	59.27
Blanket assembly dimensions (at 20°C), cm	
Number of pins per assembly	19

Outer cladding diameter	1.2522
Inner cladding diameter	1.1608
Outer fuel diameter	1.1100
Pin length	139.0
Volume fractions (%)	
Depleted uranium	61.13
Stainless steel (Type 304)	17.64
Sodium	21.23
Subassembly data summary	
No. of core driver subassemblies	87
No. of control rods	8
No. of safety rods	2
No. of experimental subassemblies	5
No. of reflector subassemblies	201
No. of blanket subassemblies	330
Total No. of subassemblies in reactor	637
Configuration	Hexagonal
Assembly pitch	5.8929
Outer flat-flat distance	5.8166
Inner flat-flat distance	5.6134

4 Expected Results

The following results are expected from this benchmark;

- Core multiplication factor,
- Effective delayed neutron fraction,
- Power distribution of each subassembly including fission and gamma heat
- Fission and decay heat power for 15 minutes assuming a reactor scram at the beginning of SHRT-45R,
- Reactivity feedback coefficients:
  - Axial expansion reactivity feedback coefficient
  - Radial expansion reactivity feedback coefficient
  - Sodium density reactivity feedback coefficient
  - Doppler constant,
  - Control rod expansion reactivity feedback coefficient.

For the completeness, the summary of the applied methodologies and the computation tools are also requested. In this benchmark, all reactivity feedback coefficients are defined by the change in reactivity per unit change in temperature (pcm/K),

$$\alpha = \frac{\partial \rho}{\partial T}, \tag{4.1}$$

where ρ is the total reactivity of the reactor, T is the temperature of the reactor component under investigation (i.e., fuel, coolant, or structure). The Doppler constant (pcm) is calculated by assuming that the Doppler effect is inversely proportional to fuel temperature T_f in Kelvin,

$$\alpha^{\mathrm{Doppler}} = \frac{\Delta \rho}{\ln{(T_f'/T_f)}} \text{ (pcm)} \tag{4.2}$$

where T_f and T_f' are average fuel temperatures at nominal and perturbed states, respectively. The average fuel temperature at the nominal condition was assumed to be 487 ^{o}C.

Appendix A: Core Subassembly Geometry

In this Appendix, Figures A.1-26 show elevation and plan sections for all the remaining types of subassemblies described in Chapter 3. Schematic figures for the core drivers, dummy, radial reflector, outer blanket, control/safety rods, instrumented subassemblies, and experimental subassemblies are provided in this Appendix. It should be noted that the schematics presented in the figures in the following sections describing the subassemblies are not to scale and are engineering simplifications of the original blueprints.

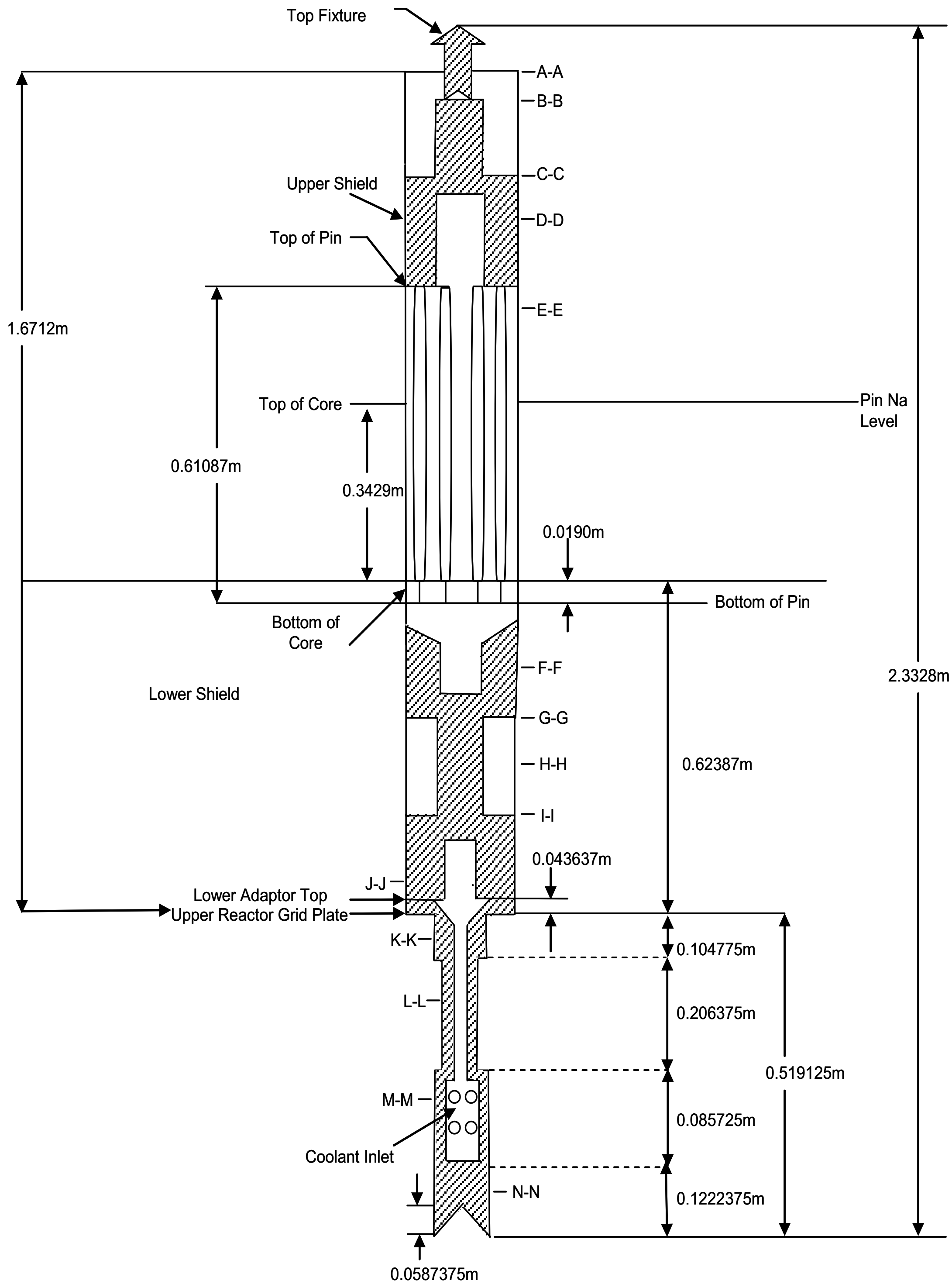

Figure A.1. MARK-II AI (Including HFD) Core Driver Elevation Section

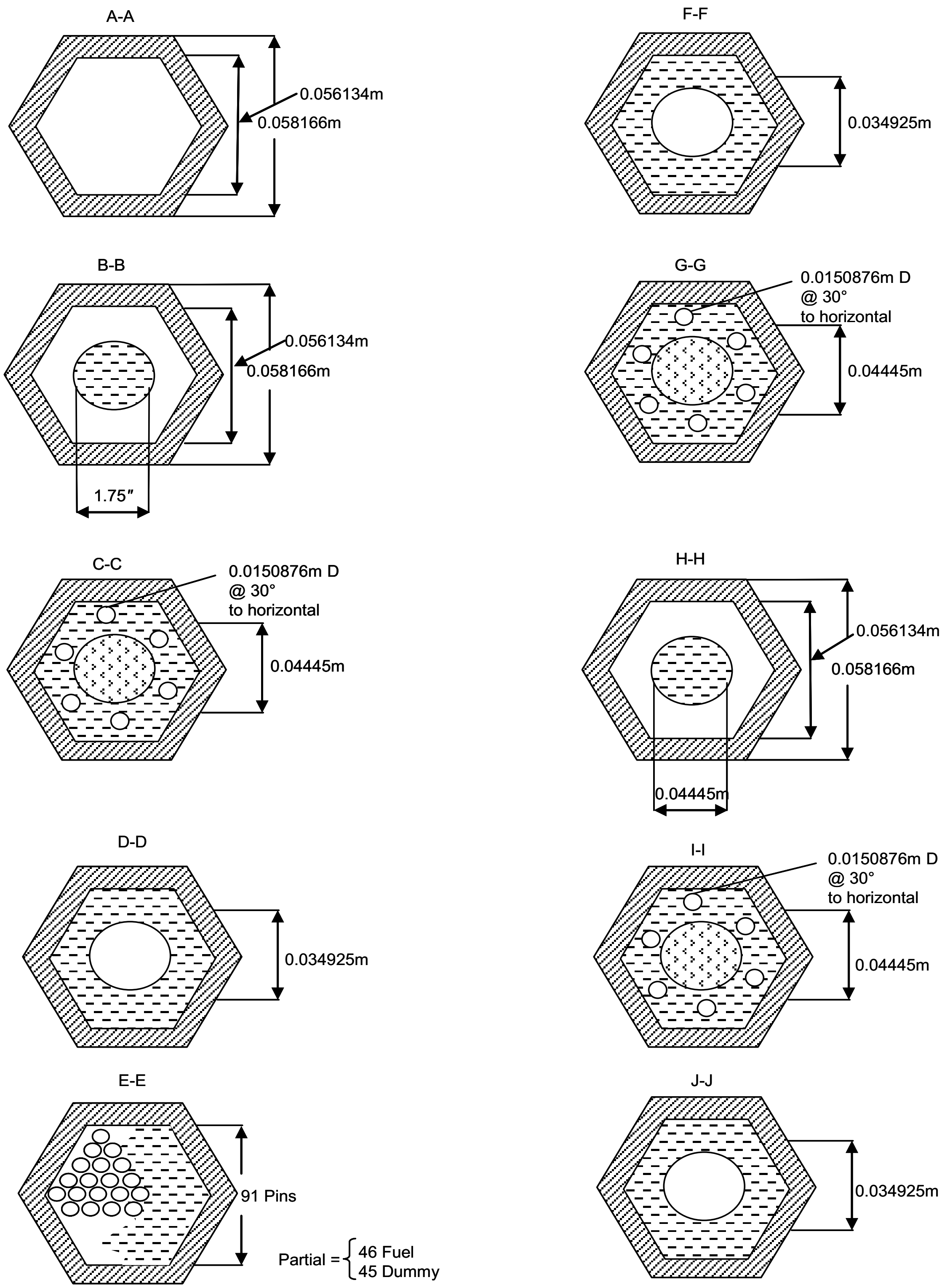

Figure A.2. MARK-II AI (Including HFD) Core Driver Plane Sections

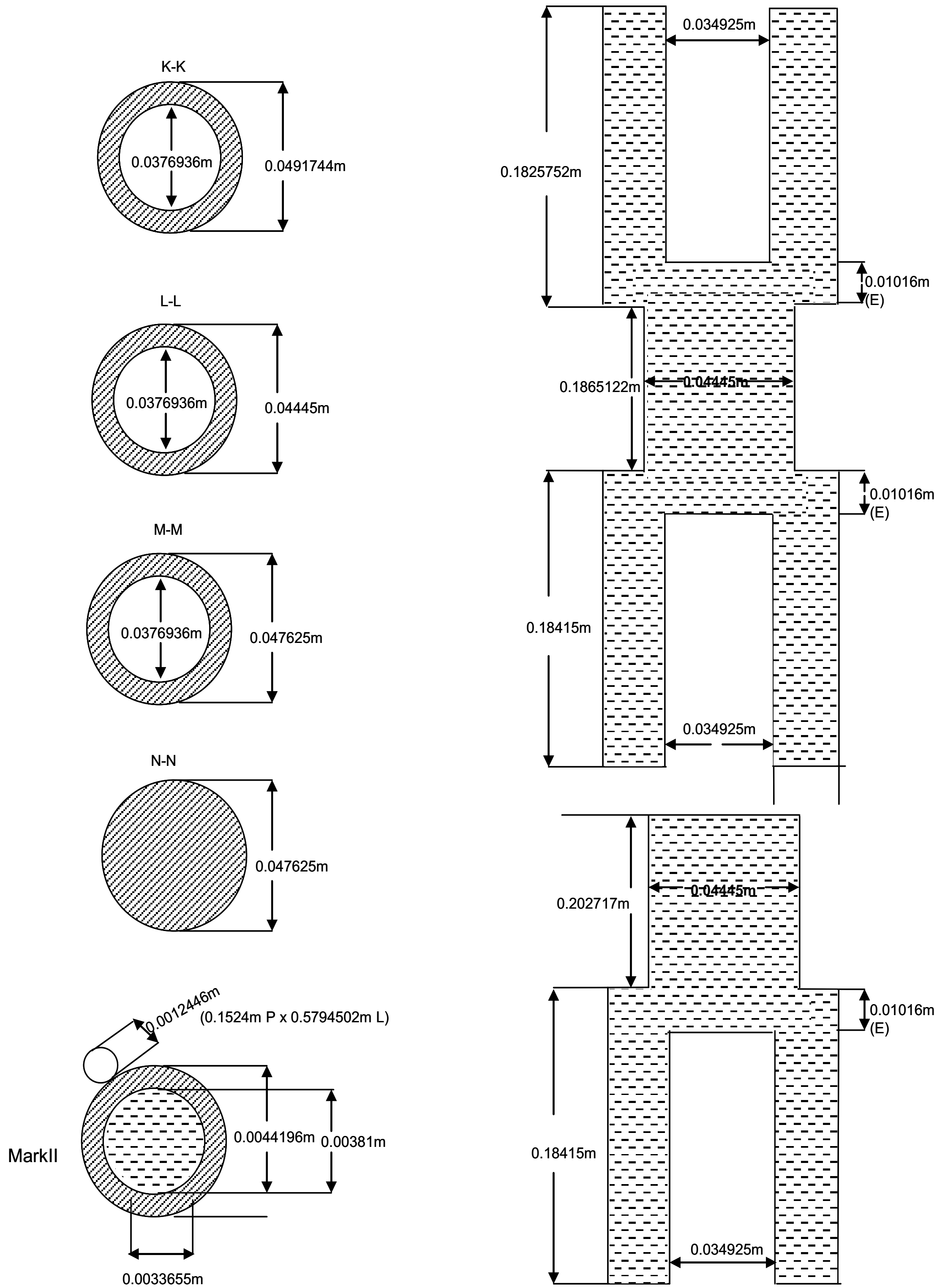

Figure A.3. MARK-II AI (Including HFD) Core Driver Elevation and Plane Sections

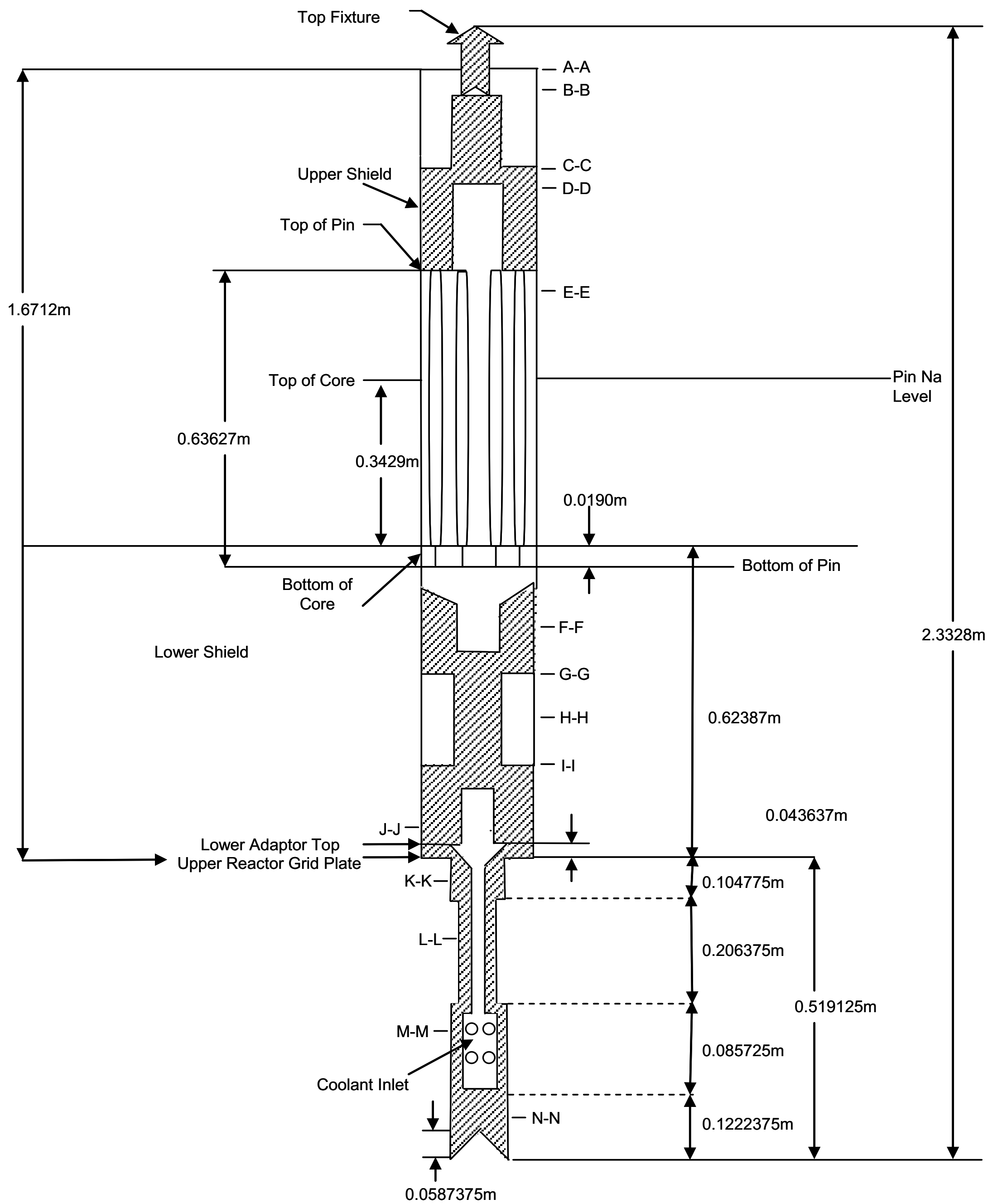

Figure A.4. MARK-IIA Core Driver (Including HFD) Elevation Section

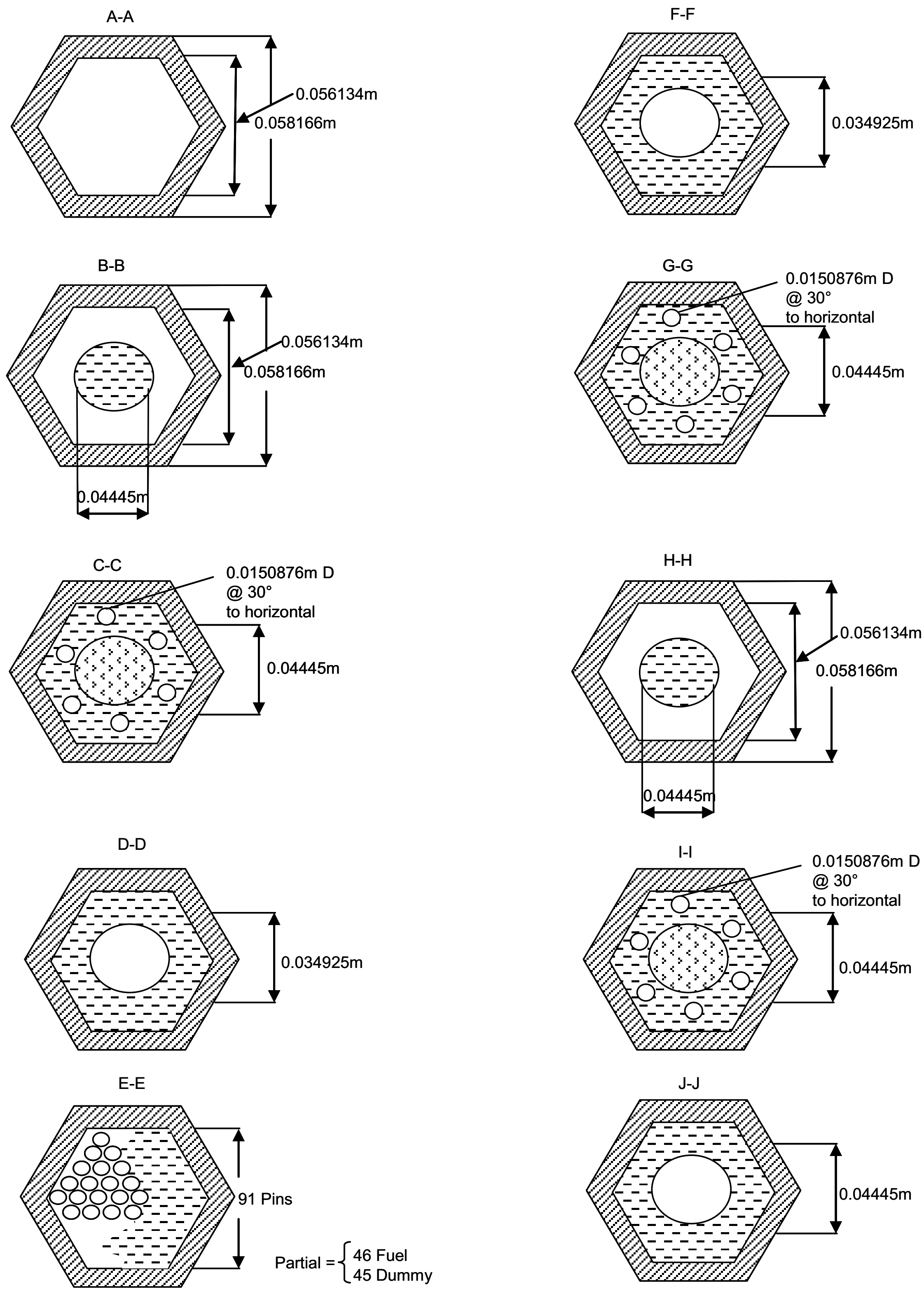

Figure A.5. MARK-IIA Core Driver (Including HFD) Plane Sections

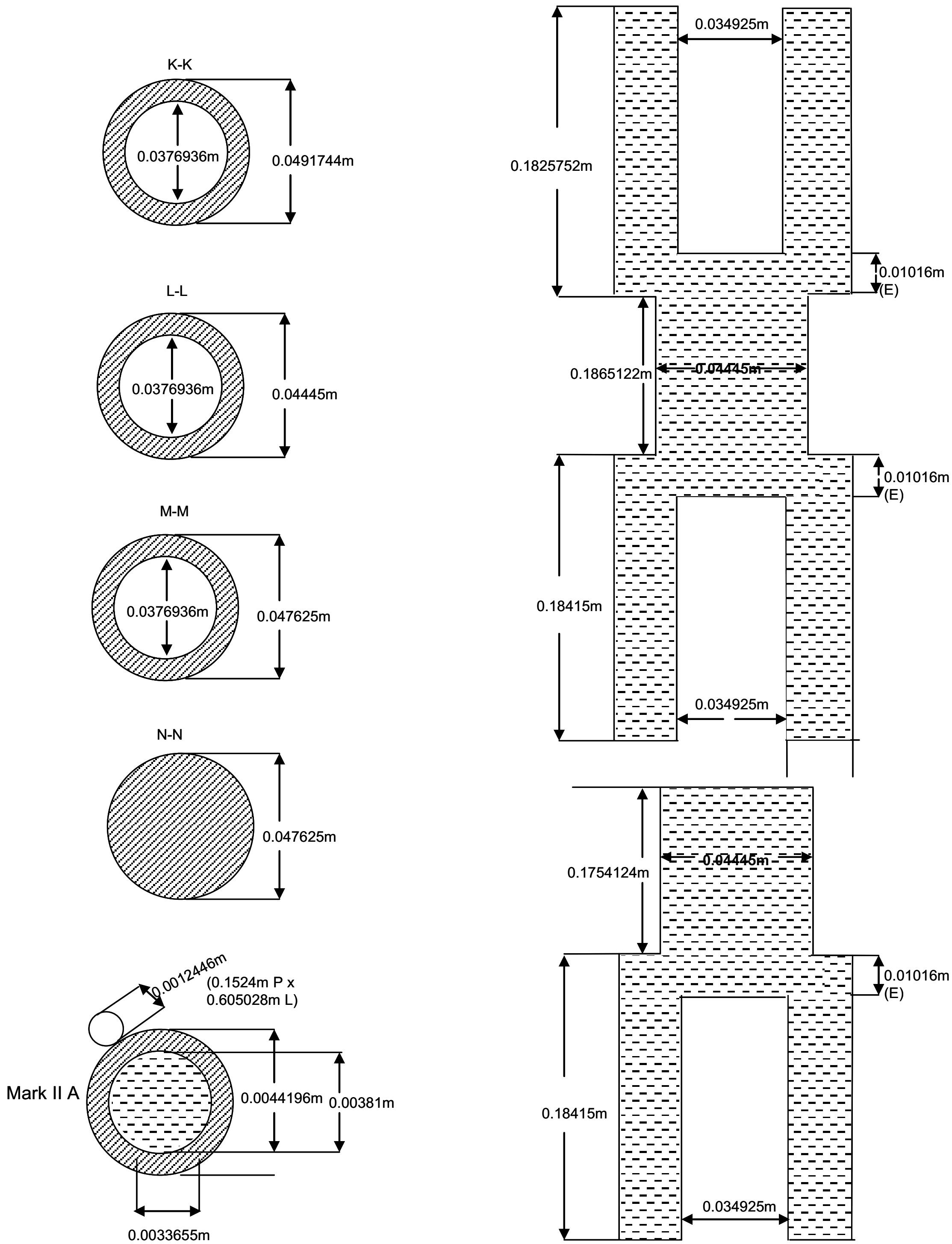

Figure A.6. MARK-IIA Core Driver (Including HFD) Elevation and Plane Sections

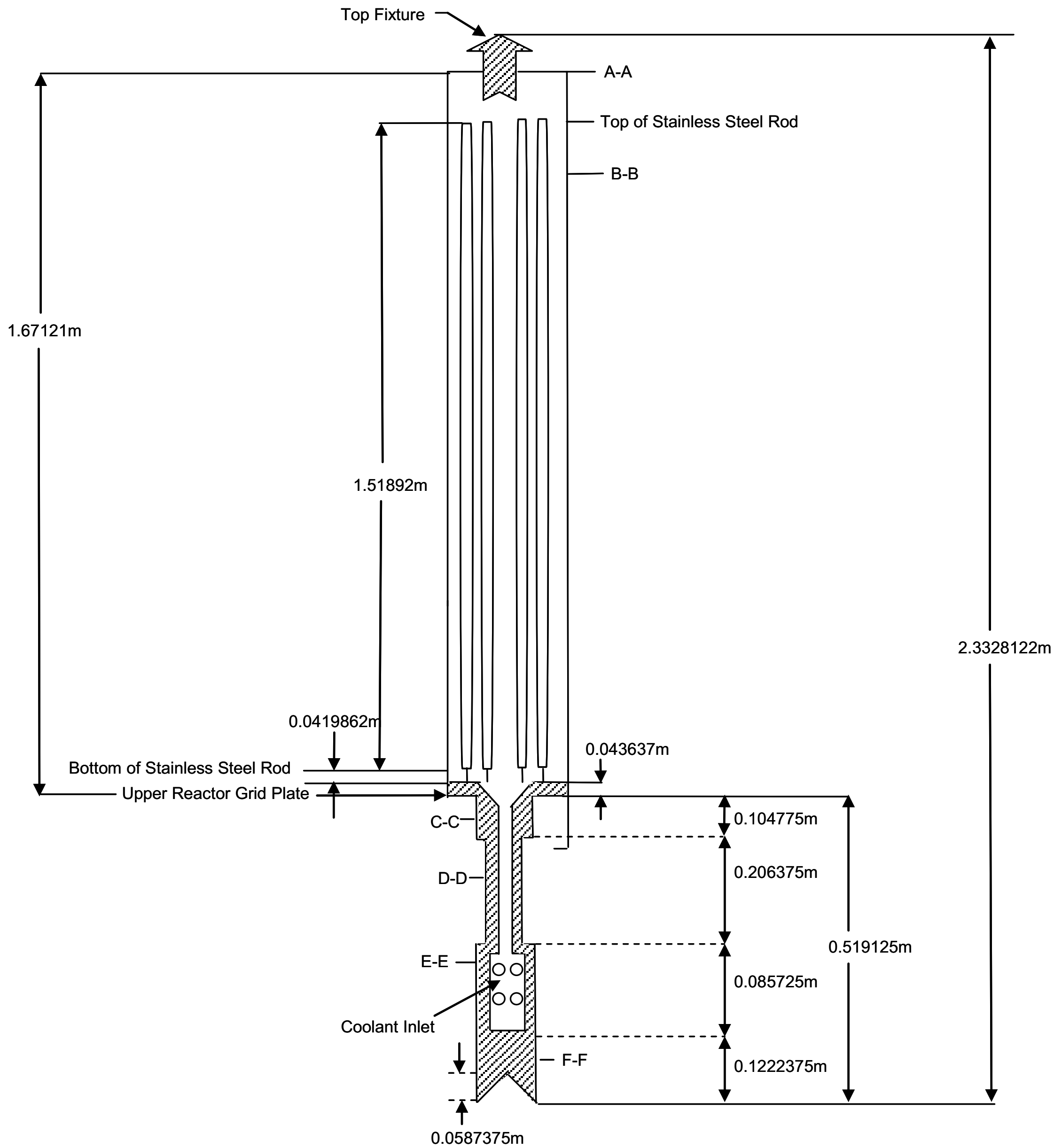

Figure A.7. Core Dummy Elevation Section

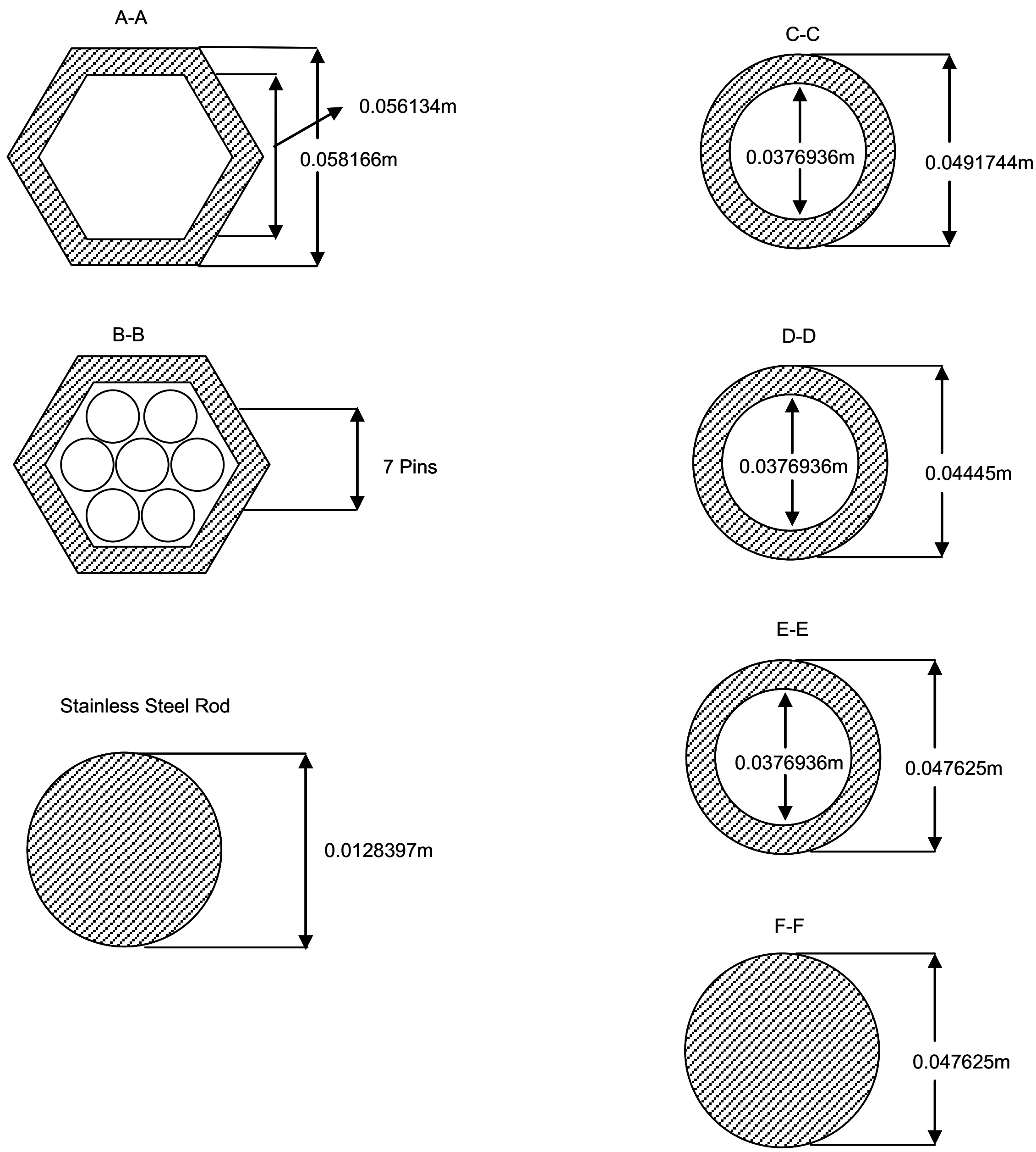

Figure A.8. Core Dummy Plane Sections

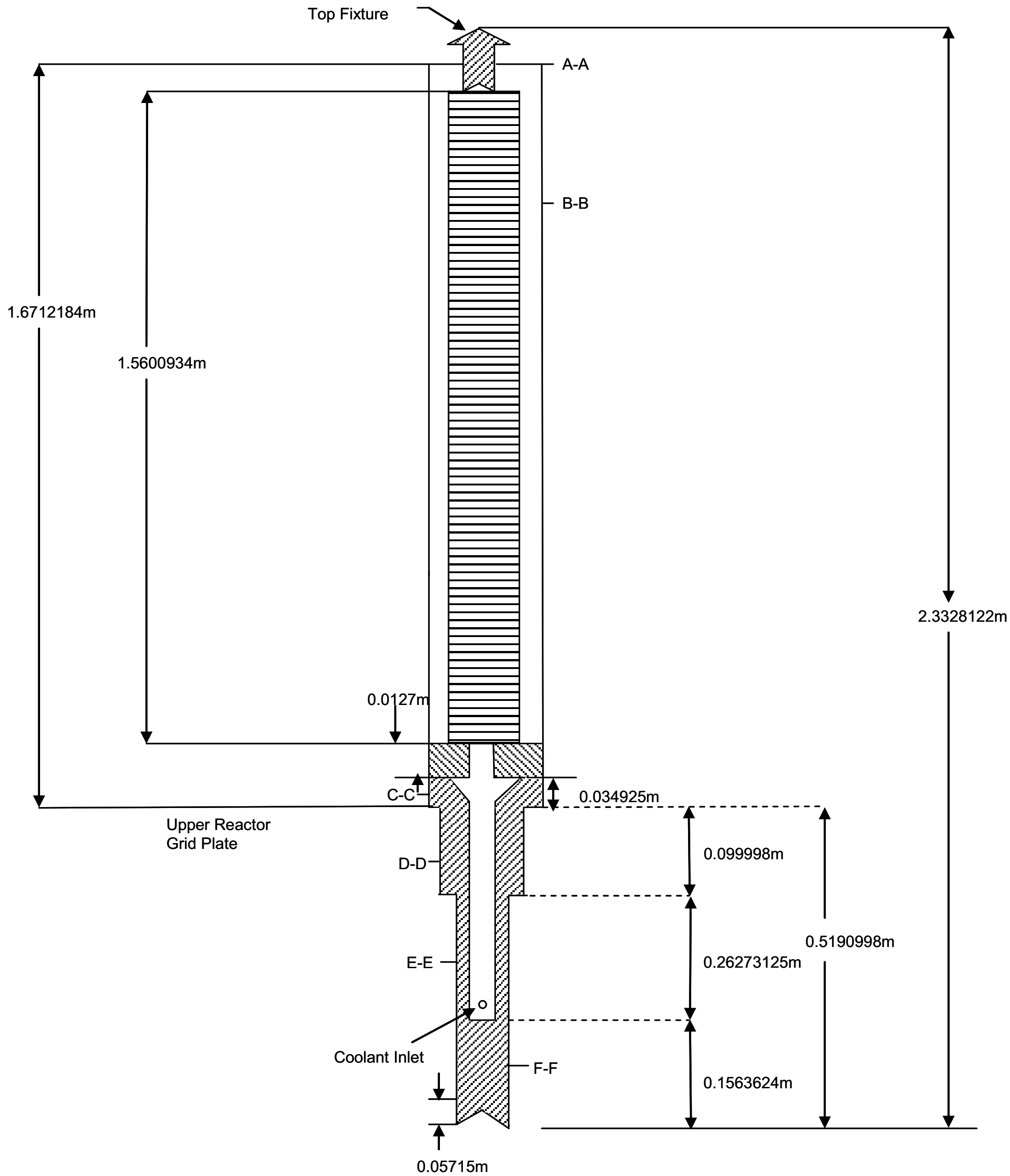

Figure A.9. Stainless Steel Radial Reflector Elevation Section

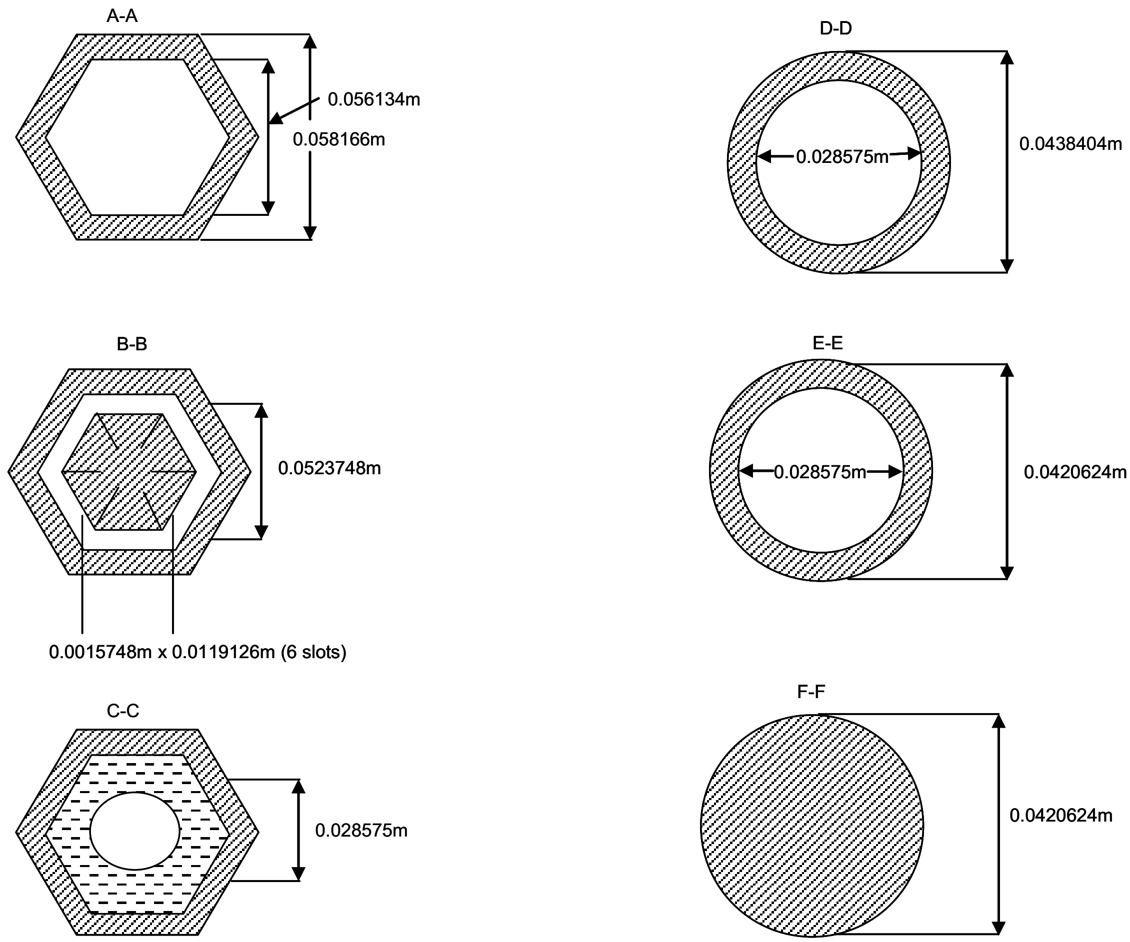

Figure A.10. Stainless Steel Radial Reflector Plane Sections

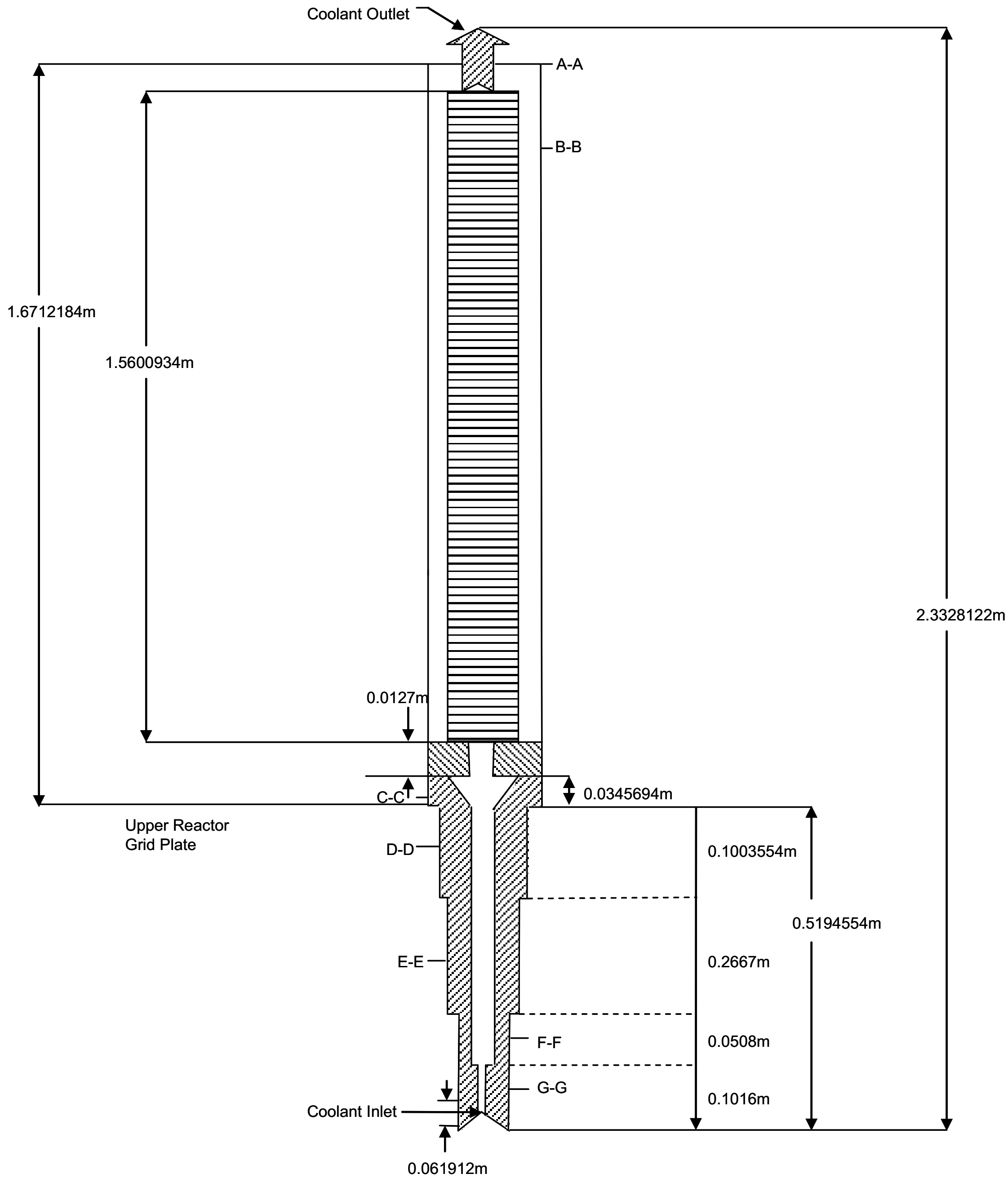

Figure A.11. Stainless Steel Radial Reflector Elevation Section

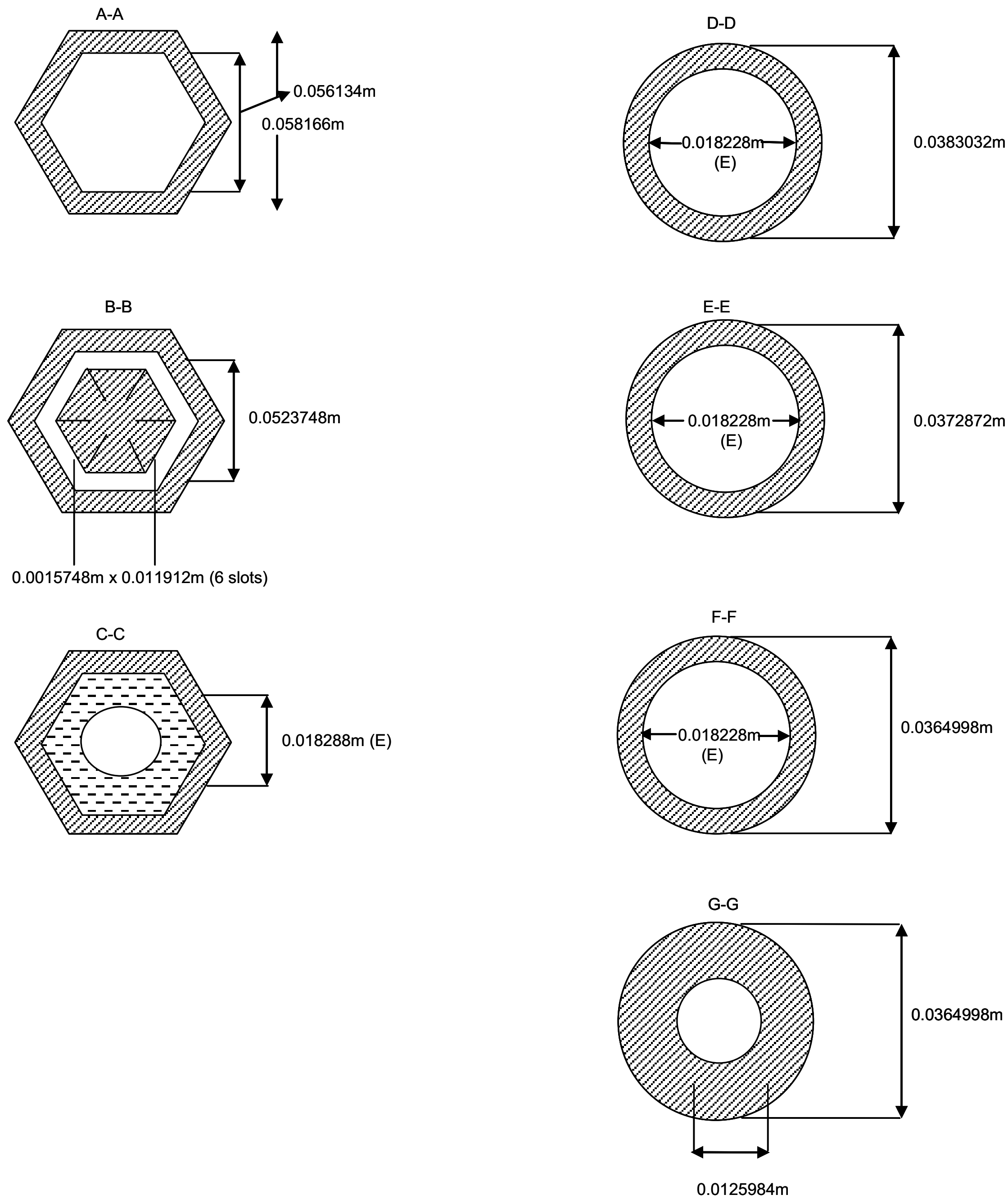

Figure A.12. Stainless Steel Radial Reflector Plane Sections

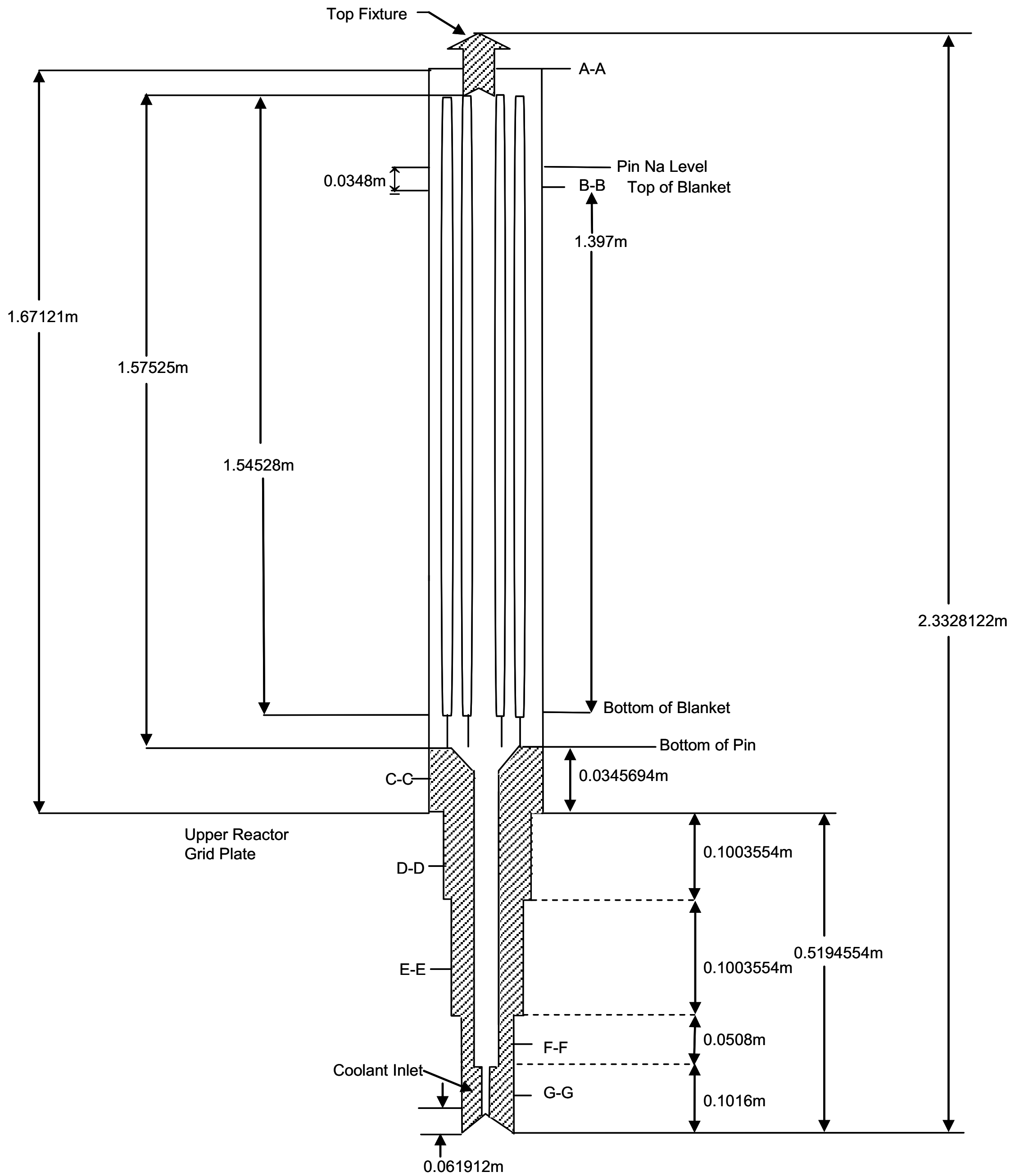

Figure A.13. Uranium Outer Blanket Elevation Section

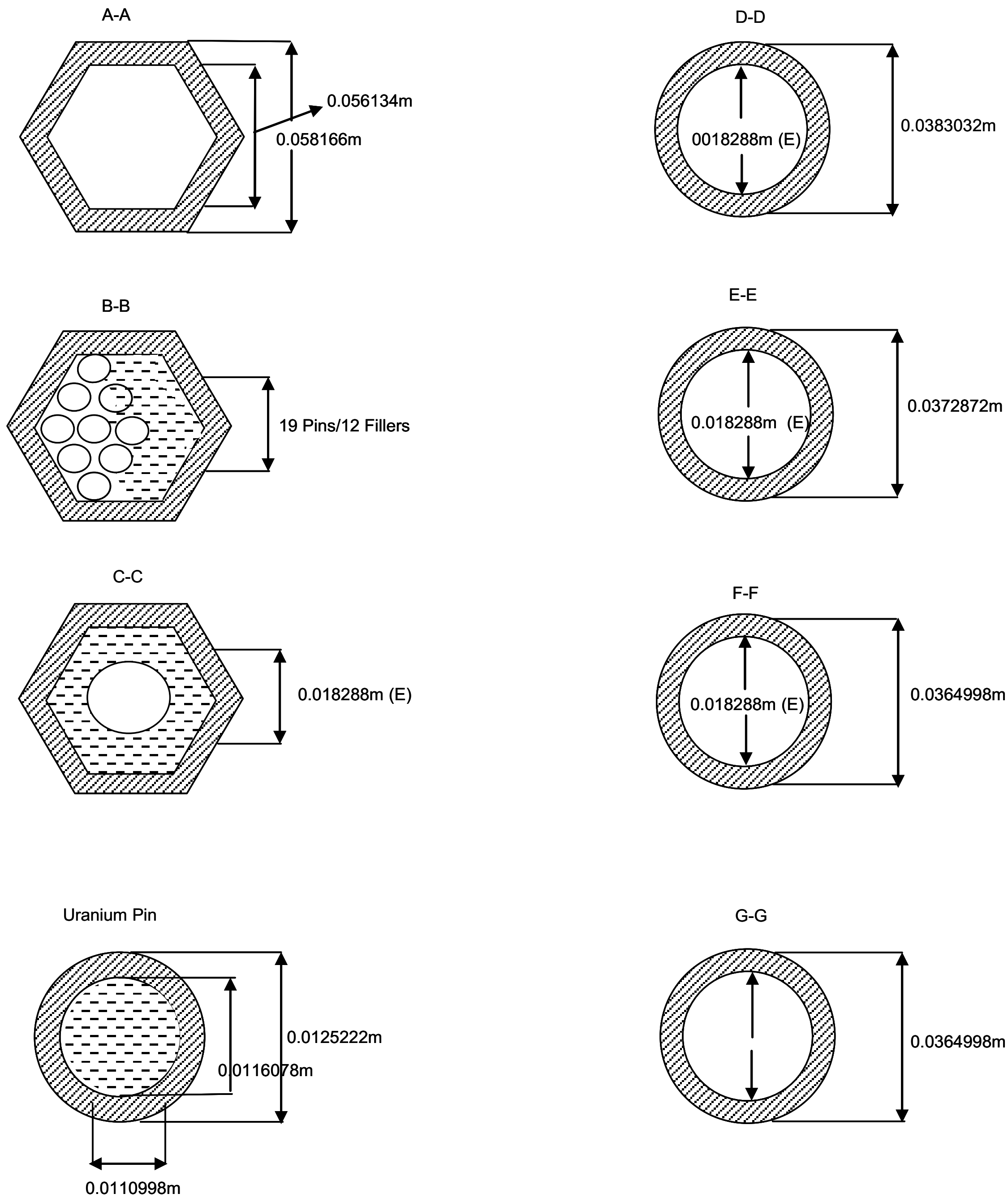

Figure A.14. Uranium Outer Blanket Plane Sections

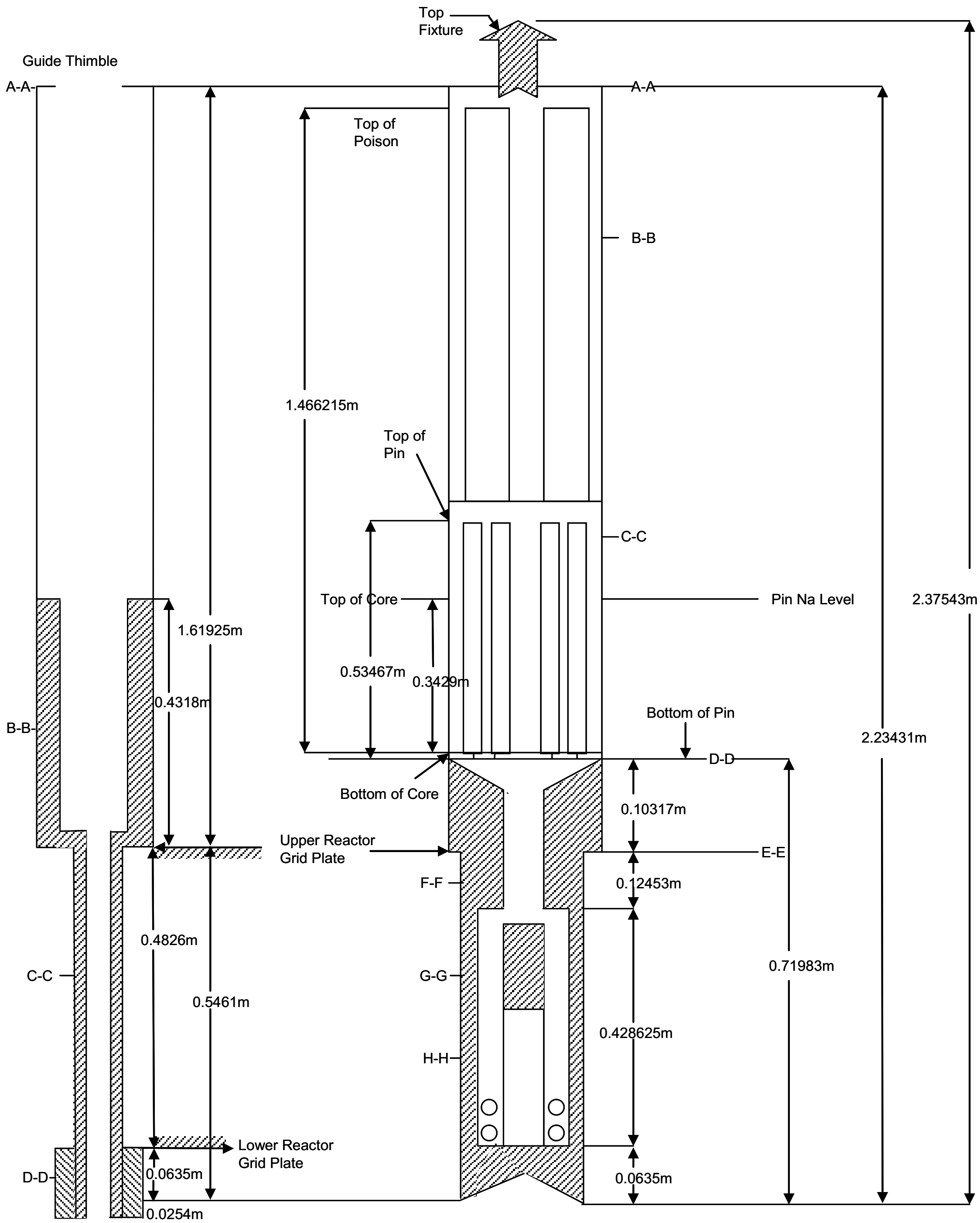

Figure A.15. High-Worth Control Rod Elevation Section

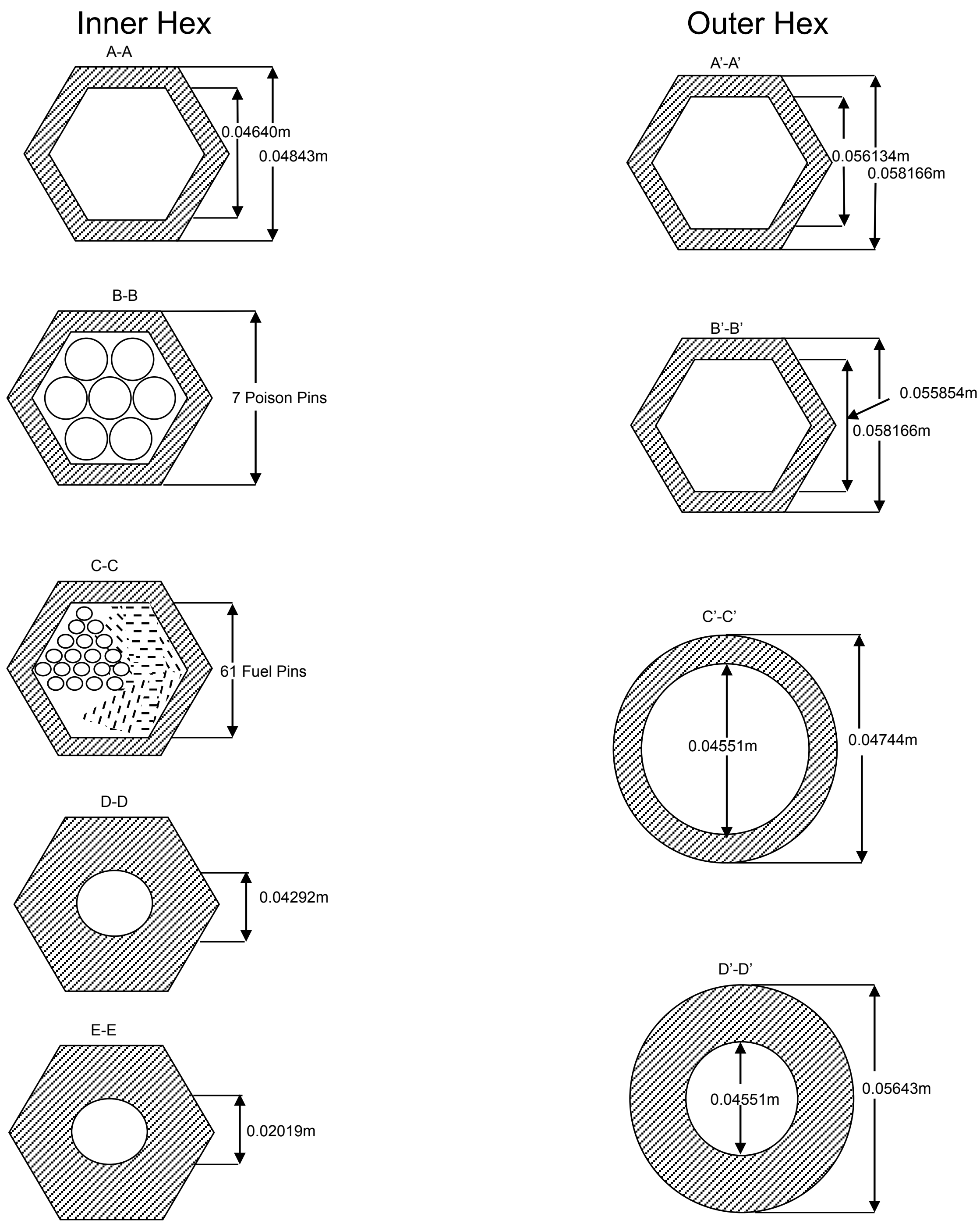

Figure A.16. High-Worth Control Rod Plane Sections

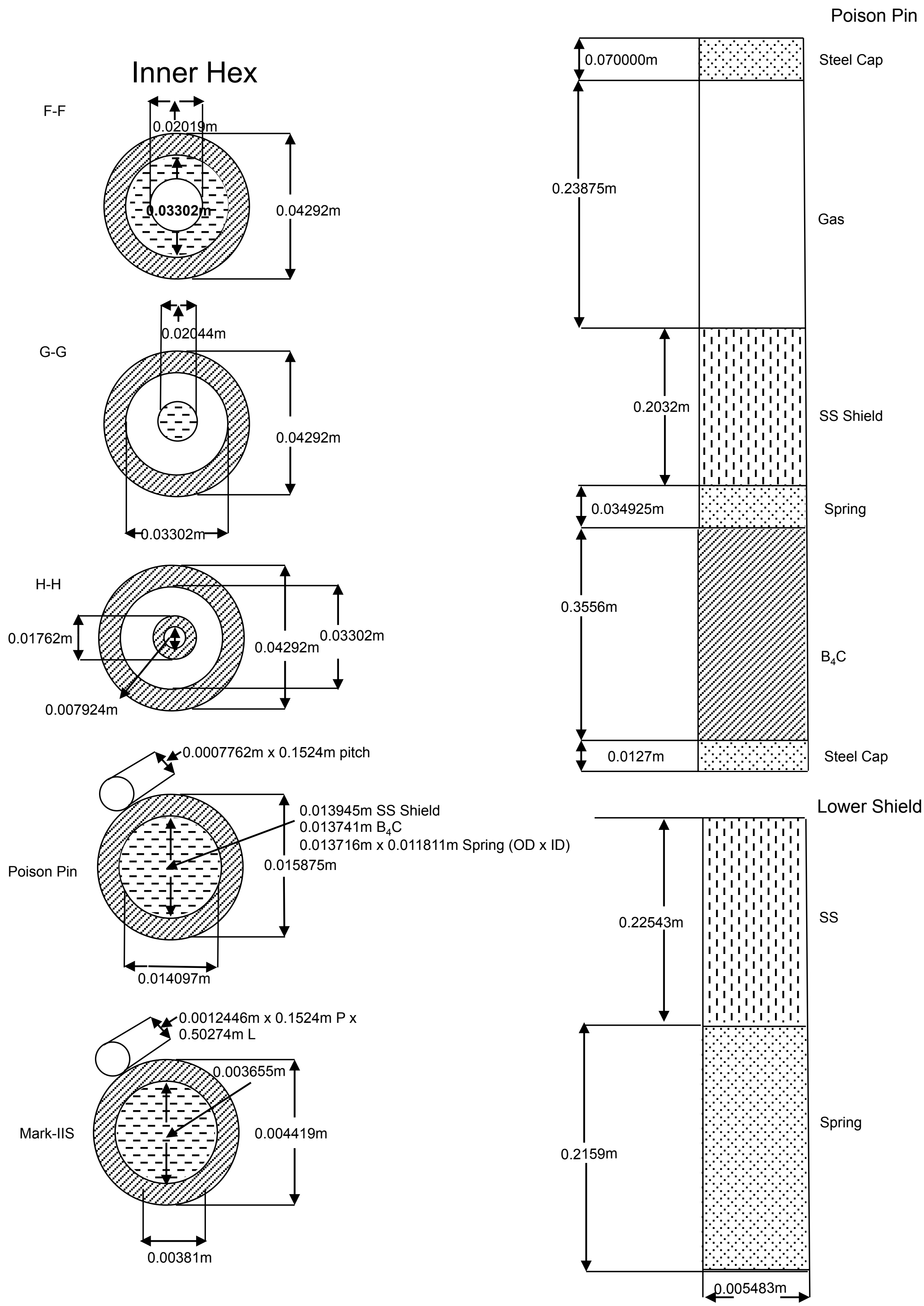

Figure A.17. High-Worth Control Rod Elevation and Plane Sections

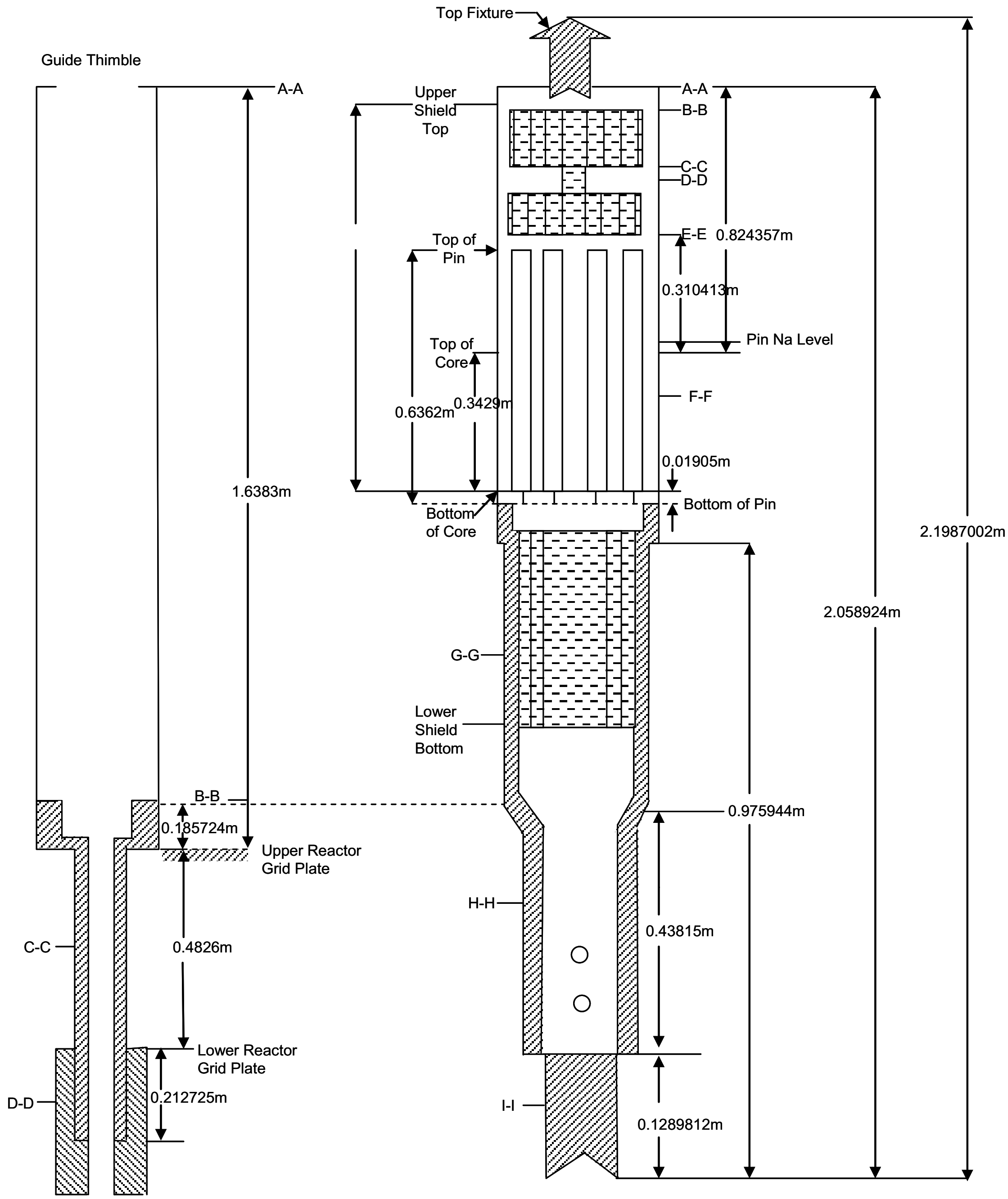

Figure A.18. Safety Rod Elevation Section

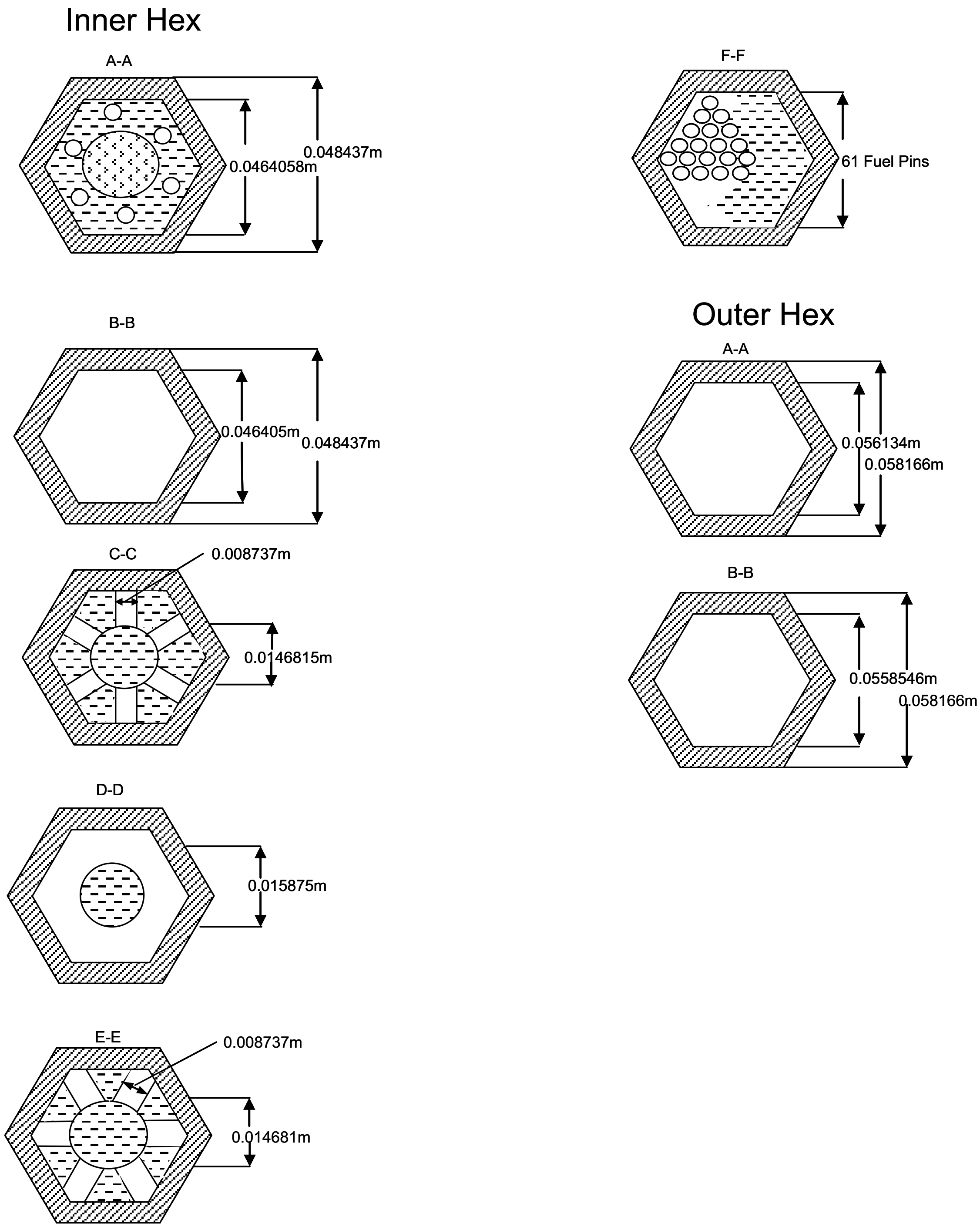

Figure A.19. Safety Rod Plane Sections

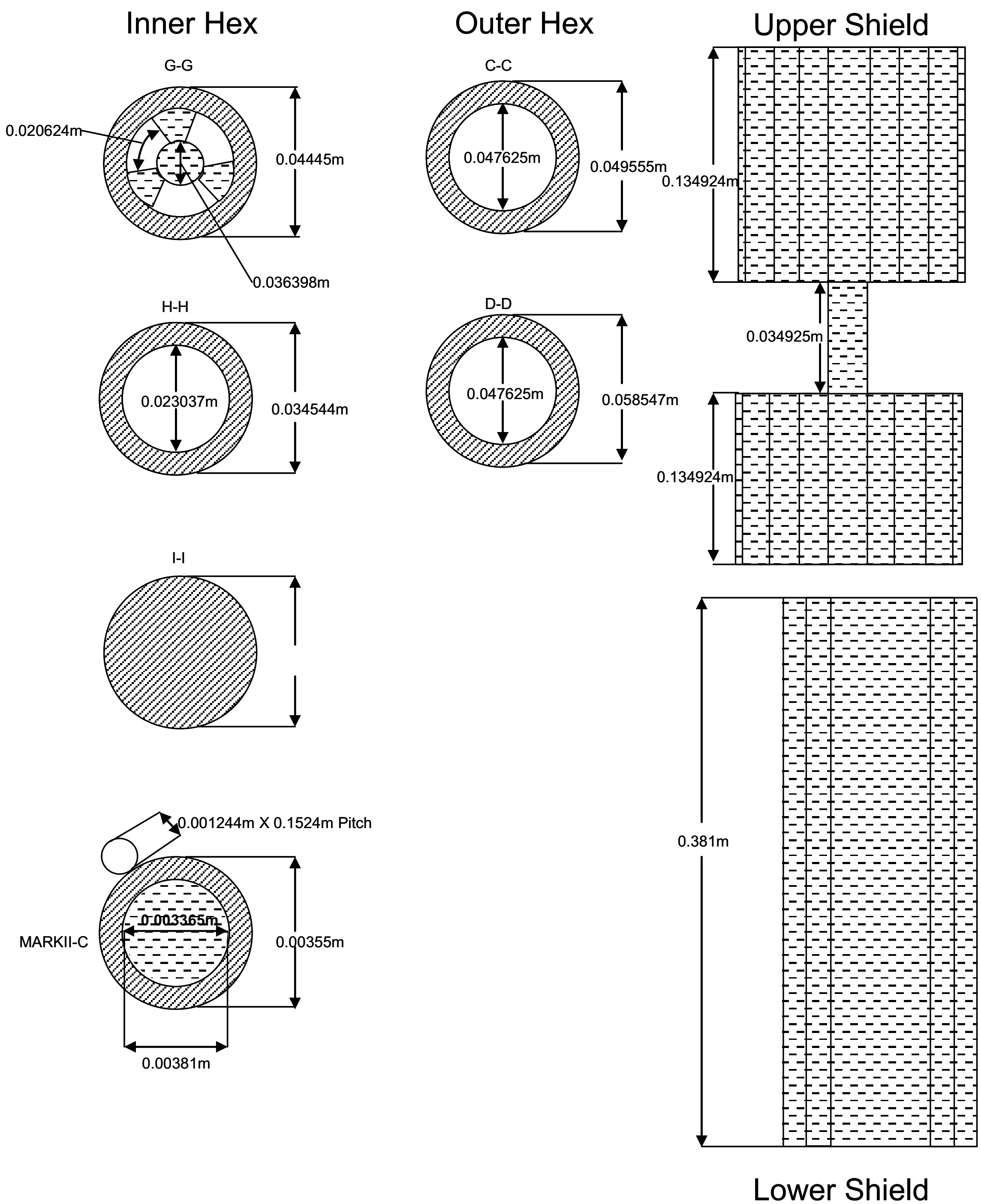

Figure A.20. Safety Rod Elevation and Plane Sections

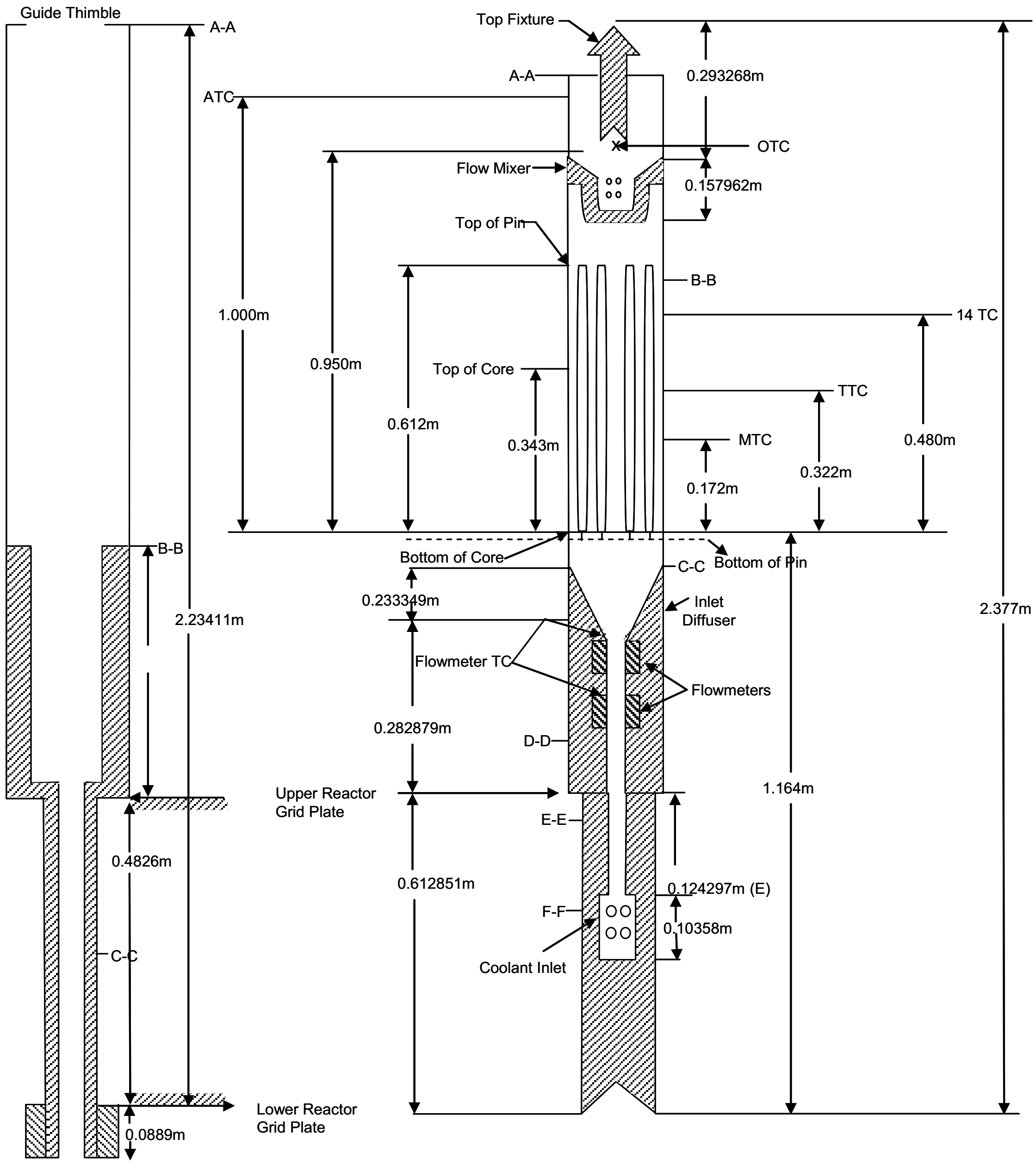

Figure A.21. XX09 Instrumented Elevation Section

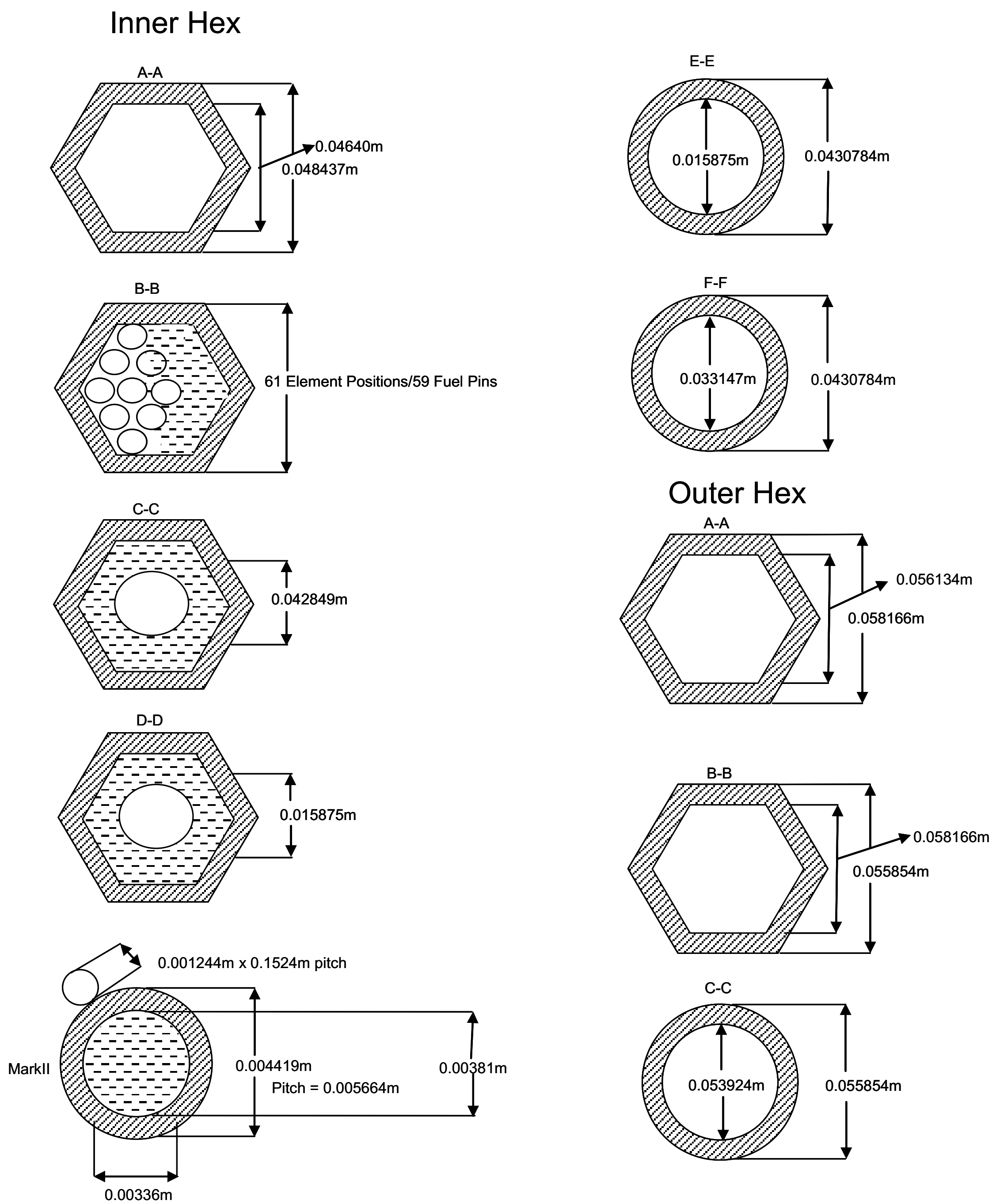

Figure A.22. XX09 Instrumented Plane Sections

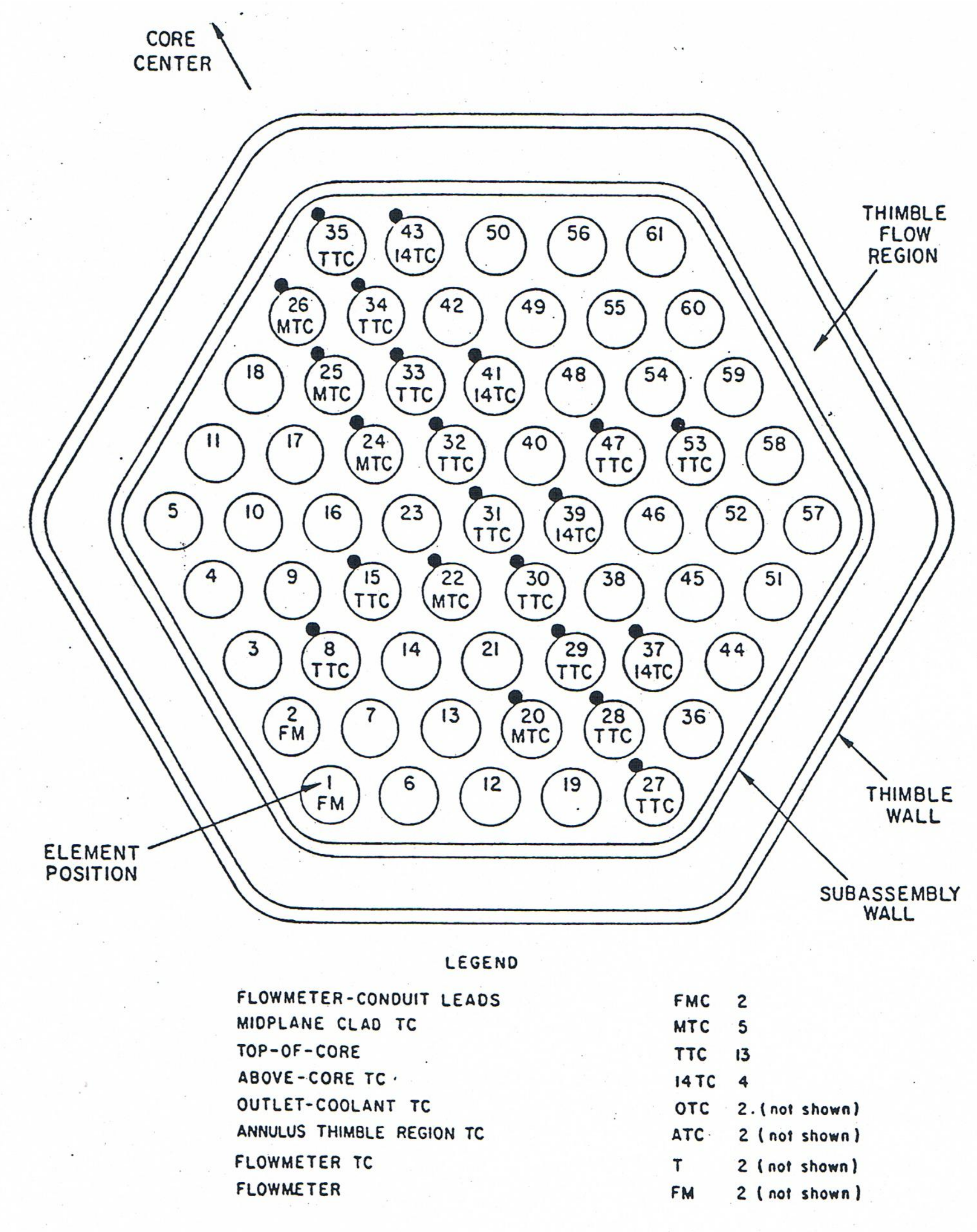

Figure A.23. XX09 Instrumented Instrument Loading

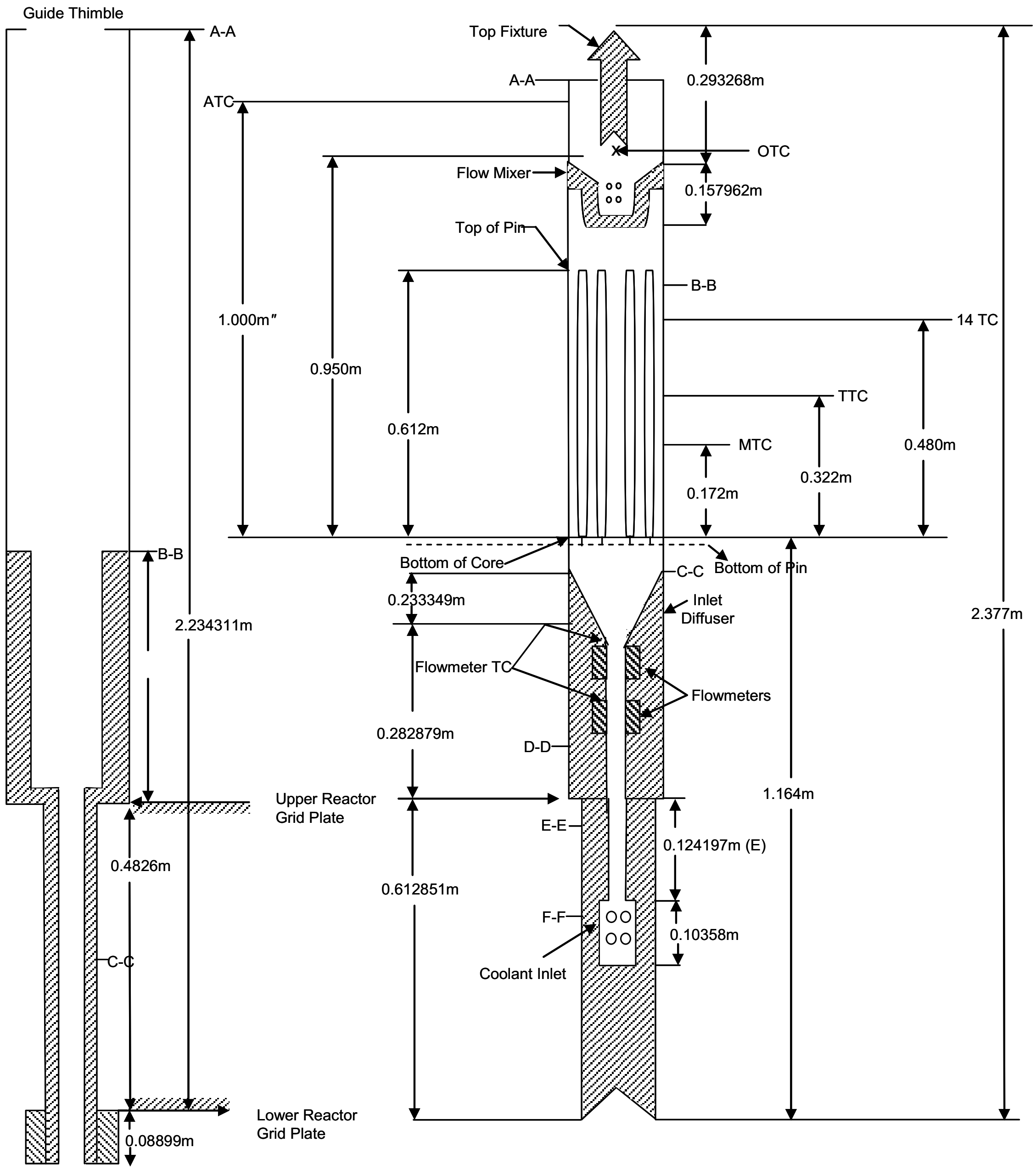

Figure A.24. XX10 Instrumented Elevation Section

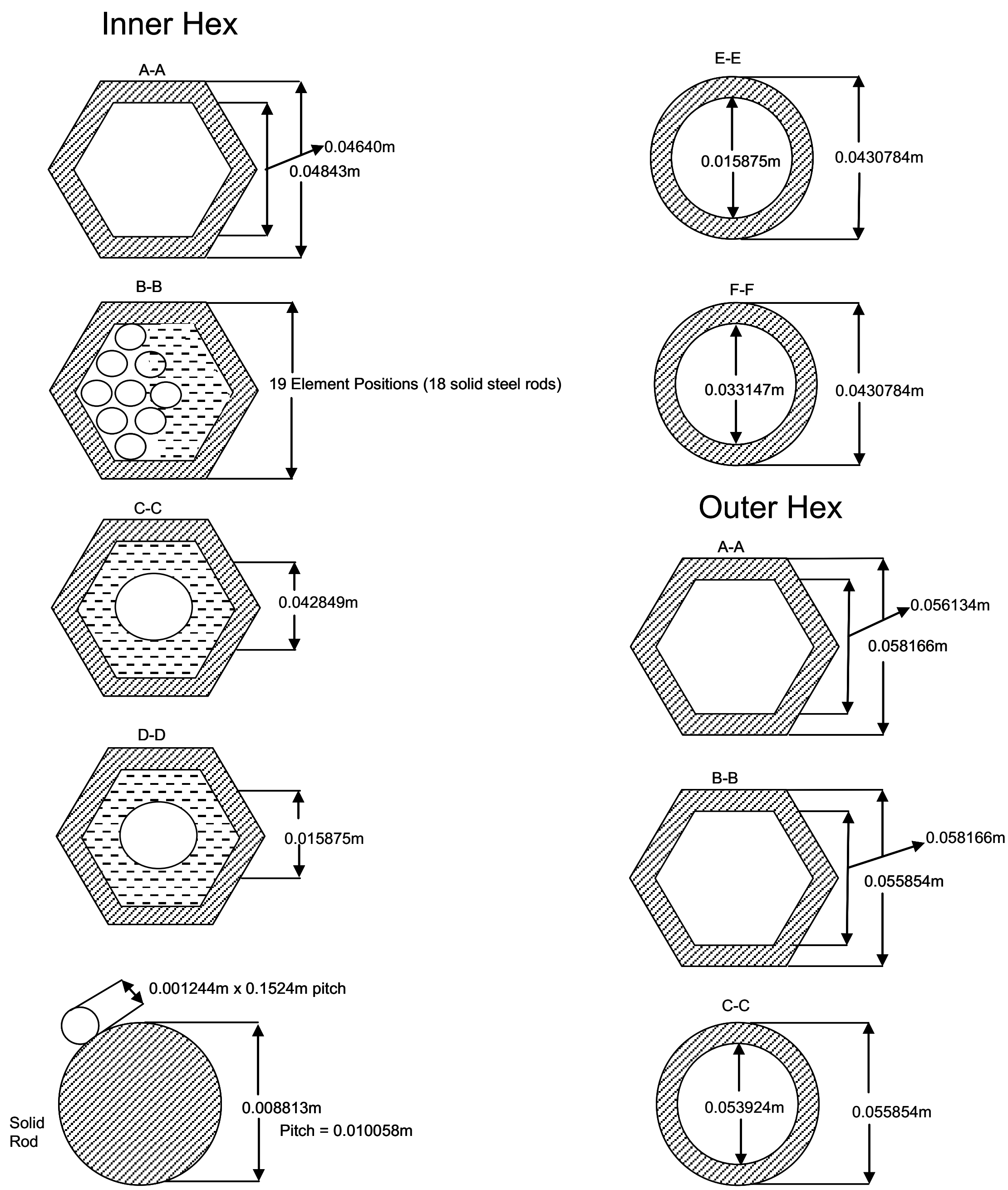

Figure A.25. XX10 Instrumented Plane Sections

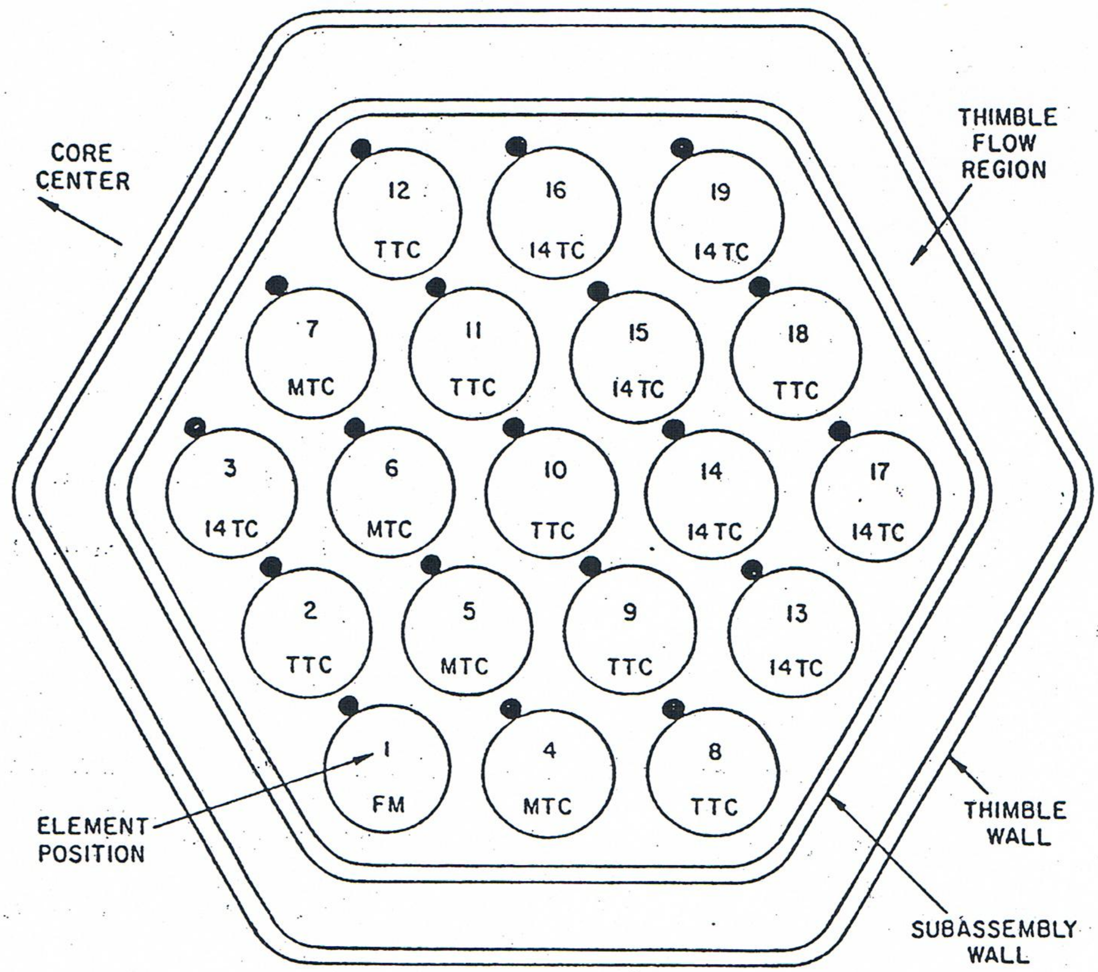

LEGEND

FLOWMETER-CONDUIT LEAD	FM	1
MIDPLANE SPACER-WIRE THERMOCOUPLE	MTC	4
TOP-OF-CORE SPACER-WIRE THERMOCOUPLE	TTC	7
ABOVE-CORE SPACER-WIRE THERMOCOUPLE	14TC	7
OUTLET-COOLANT THERMOCOUPLE	OTC	2 (not shown)
ANNULUS THIMBLE THERMOCOUPLE	ATC	2 (not shown)
EXTENSION TUBE THERMOCOUPLE	ETC	2 (not shown)
FLOWMETER THERMOCOUPLE	T	2 (not shown)
FLOWMETER	F	2 (not shown)

Figure A.26. XX10 Instrumented Instrument Loading

Appendix B: Isotopic Compositions of core Assemblies

Similar to Table 3.2.1 in Chapter 3 which lists isotopic fuel compositions of the central core assembly at position 1A1, Appendix B provides the homogenized isotopic compositions for all core assemblies. This data is presented as an electronic appendix in the .csv file ANL-ARC-228_Appendix_B_Fuel_Isotopic_Compositions.csv that accompanies this report.

Depleted isotopic compositions are presented for three axial zones at 20ºC. The three fuel zones are equally spaced, with the zone labels 1, 2 and 3 referring to the lower, middle, and upper sections. Axial fuel swelling of 6.88% corresponding to 4.5 atomic % average core burnup has been assumed in the fuel heights that were used in the calculation of these homogenized number densities.

Appendix C: Isotopic Compositions of Blanket Assemblies

Similar to Table 3.2.1 in Chapter 3 which lists isotopic fuel compositions of the central core assembly at position 1A1, Appendix B provides the homogenized isotopic compositions for all blanket assemblies. This data is presented as an electronic appendix in the .csv file ANL-ARC-228_Appendix_C_Blanket_Isotopic_Compositions.csv that accompanies this report.

Depleted isotopic compositions are presented for three axial zones at 20ºC. Isotopic compositions for the blanket assemblies are also presented in three zones. Zone 1 corresponds with the region below the bottom elevation of the active fuel in the driver assemblies and Zone 3 corresponds with the region above the upper elevation of the active fuel in the driver assemblies. Zone 2 is in between, within the upper and lower elevations of the axially swelled core section.

References

1. Leonard J. Koch, *Experimental Breeder Reactor-II (EBR-II): An Integrated Fast Reactor Nuclear Power Station*, American Nuclear Society, 2008.
2. S. H. Fistedis, editor, The Experimental Breeder Reactor-II Inherent Safety Demonstration, reprinted from Nuclear Engineering and Design, Vol. 101, No. 1 (1987).
3. J. Ploncsik, E. C. Filewicz, G. J. Kamis and J. T. Natoce, “The Experimental Breeder Reactor (EBR-II) Instrumented Subassemblies, INSAT XX09 and XX10,” American Nuclear Society Fast, Thermal and Fusion Reactor Experiments Conference, Utah, April 12-15, 1982.

Nuclear Engineering Division
Argonne National Laboratory
9700 South Cass Avenue, Bldg. 208
Argonne, IL 60439

www.anl.gov